

# Tackling the Static Correlation Challenge with the $\Delta\text{NO}$ Method

by

Ismael A. Elayan

A Thesis Submitted to the Faculty of Graduate Studies of

The University of Manitoba

in partial fulfillment of the requirements of the degree of

Master of Science

Department of Chemistry

University of Manitoba

Winnipeg, Manitoba, Canada

© 2020 by Ismael A. Elayan

# Contents

<b>Contents</b>	<b>i</b>
<b>List of Figures</b>	<b>iii</b>
<b>List of Tables</b>	<b>iv</b>
<b>List of Abbreviations</b>	<b>v</b>
<b>1 Introduction</b>	<b>1</b>
1.1 Theoretical Background . . . . .	2
1.1.1 The Schrödinger Equation . . . . .	2
1.1.2 The Variation Principle . . . . .	3
1.1.3 The Born–Oppenheimer Approximation . . . . .	4
1.1.4 Hartree–Fock Theory . . . . .	5
1.1.5 Electron Correlation . . . . .	8
1.1.6 Density Functional Theory . . . . .	9
1.1.7 Post Hartree–Fock Methods . . . . .	12
1.2 Hartree–Fock Dissociation of Molecules . . . . .	15
<b>References</b>	<b>19</b>
<b>2 Performance of <math>\Delta</math>NO Towards Statically Correlated Hydrogen Clusters</b>	<b>21</b>
2.1 Introduction . . . . .	21

2.2	Theory . . . . .	24
2.2.1	The $\Delta$ NO Method . . . . .	24
2.3	Methods . . . . .	30
2.4	Results and Discussion . . . . .	31
2.5	Conclusions . . . . .	39
	<b>References</b>	<b>41</b>
	<b>3 Summary and Future work</b>	<b>51</b>
	<b>A Appendix</b>	<b>54</b>

# List of Figures

1.1	Description of an RHF singlet state, ROHF and UHF doublet states. Lines indicate the energy of spatial orbitals. . . . .	16
1.2	Dissociation of H <sub>2</sub> as a function of bond length. Selected basis set cc-pVTZ.	17
2.1	Challenging systems of H clusters. From top left, H <sub>3</sub> C <sub>∞v</sub> , H <sub>4</sub> ; D <sub>∞h</sub> , D <sub>4h</sub> and D <sub>2h</sub> /D <sub>4h</sub> . R in Å. . . . .	31
2.2	Potential energy surface of H <sub>3</sub> as a function of R (Å). . . . .	32
2.3	Change in occupation numbers of statically correlated NOs of H <sub>3</sub> as a function of R (Å). . . . .	33
2.4	Potential energy surface of H <sub>4</sub> as a function of R (Å). . . . .	34
2.5	Potential energy surface of square H <sub>4</sub> (D <sub>4h</sub> ) as a function of R (Å). . . . .	35
2.6	Potential energy surface of H <sub>4</sub> (D <sub>2h</sub> /D <sub>4h</sub> ), top left R = 0.8, 1.0 Å bottom left R = 1.2, 1.5 Å, as a function of θ. . . . .	36
2.7	Potential energy surface of H <sub>4</sub> (D <sub>2h</sub> /D <sub>4h</sub> ), top left counter clockwise R = 1.7, 2.2, 3.0 Å, as a function of θ. . . . .	38
A.1	Change of occupation numbers of statically correlated NOs of H <sub>4</sub> as a function of R. . . . .	54
A.2	Change of occupation numbers of statically correlated NOs of square H <sub>4</sub> (D <sub>4h</sub> ) as a function of R. . . . .	55
A.3	Change in occupation numbers of statically correlated NOs of H <sub>4</sub> (D <sub>2h</sub> /D <sub>4h</sub> ) as a function of θ, R = 3.0 Å. . . . .	55

# List of Tables

2.1	Equilibrium bond lengths ( $\text{\AA}$ ) and minimum energies (hartree) of different hydrogen systems. . . . .	32
2.2	Dissociation energies ( $\text{kJ mol}^{-1}$ ) of different hydrogen systems. . . . .	33
2.3	$\Delta E$ values ( $\text{kJ mol}^{-1}$ ) as a function of $\theta$ for $\text{H}_4$ ( $D_{2h}/D_{4h}$ ). . . . .	37
2.4	The difference in absolute energies at $\theta = 90^\circ$ and $70^\circ$ ( $\text{kJ mol}^{-1}$ ) for $\text{H}_4$ ( $D_{2h}/D_{4h}$ ). Basis set aug-cc-pVDZ. . . . .	39
A.1	Absolute energy values (hartree) for $\text{H}_4$ ( $D_{2h}/D_{4h}$ ) at different $\theta$ and $R$ values. . . . .	56
A.2	The difference in absolute energies at $\theta = 90^\circ$ and $70^\circ$ ( $\text{kJ mol}^{-1}$ ) for $\text{H}_4$ ( $D_{2h}/D_{4h}$ ). . . . .	57

# List of Abbreviations

$\theta$  Angle

$D_e$  Dissociation energy

$R$  Bond length

$R_e$  Equilibrium bond length

1-RDM One-electron reduced density matrix

2-RDM Two-electron reduced density matrix

CASPT2 complete active space second order perturbation theory

CASSCF complete active space self-consistent field

CC Coupled-cluster

CCS Coupled-cluster with single excitations

CCSD Coupled-cluster with single and double excitations

CCSD(T) Coupled-cluster with single, double, and perturbed triple excitations

CCSDT Coupled-cluster with single, double, and triple excitations

CCSDTQ Coupled-cluster with single, double, triple, and quadruple excitations

CFT Cumulant functional theory

CI Configuration interaction

CIS Configuration interaction with single excitations

CISD Configuration interaction with single and double excitations

CISDT Configuration interaction with single, double, and triple excitations

CS Colle-Salvetti

DFT Density functional theory

DMFT Density-matrix functional theory

HF Hartree–Fock

HSC High-spin correction

MC-PDFT Multiconfiguration pair-density functional theory

MOs Molecular orbitals

MP Møller–Plesset

MRCI Multireference configuration interaction

MRSCF Multireference self-consistent field

NOFT Natural orbital functional theory

NOs Natural orbitals

OF Opposite-spin exponential-cusp and Fermi-hole correction

ONs Occupation numbers

pCCD Pair coupled cluster doubles

PES Potential energy surface

PNOF Piris natural orbital functional

PT2 Second order perturbation theory

RDM Reduced density matrix

RHF Restricted Hartree–Fock

ROHF Restricted open-shell Hartree–Fock

SCF Self-consistent field

TDDFT Time-dependent density functional theory

UHF Unrestricted Hartree–Fock

# Abstract

The static correlation challenge, which results due to the degeneracy of molecular orbitals in a system, is still a significant obstacle to electronic structure methods. This work investigates hydrogen clusters in arrangements with particularly significant amounts of static correlation using a cumulant functional theory,  $\Delta$ NO. Analysis of the performance of  $\Delta$ NO in conjunction with the on-top dynamic correlation functionals: Colle–Salvetti (CS) and opposite-spin exponential-cusp and Fermi-hole correction (OF), shows that it performs better than functionals that describe systems with a multi-reference and also single-reference wave function. The potential energy surfaces (PESs) of  $H_3$  and  $H_4$  clusters are analyzed and compared to B3LYP, CCSD(T), and full CI. The  $H_3$  dissociation curve computed using  $\Delta$ NO is near exact. Among the challenging systems, is the  $H_4$  cluster and its rectangle ( $D_{2h}$ ) to square ( $D_{4h}$ ) geometry transition, which appears as a cusp in energy at  $\theta = 90^\circ$  on the PES for methods with an inadequate description of static correlation. The vicinity of the cusp region is the challenging part of the system, not only quantitatively but also qualitatively. The dissociation curve of square  $H_4$  ( $D_{4h}$ ) is also computed where  $\Delta$ NO calculated energies are comparable to full CI energies. The  $\Delta$ NO method effectively describes not only the linear hydrogen systems but also the  $H_4$   $D_{2h}/D_{4h}$  transition, and produces a cusp-free PES with adequate description of occupancies.

# Dedication

*To the soul of my father,  
my mother,  
my wife.*

# Acknowledgements

I would like to thank my amazing supervisor, Dr. Joshua Hollett, for the great opportunity that he provided me to work under his supervision. Truly, with Josh, I was able to learn how to approach scientific problems with perseverance and consistency. I am indeed happy that I had the chance to work with such a kind and understanding person who believed in me and my capabilities. I also wish to extend my appreciation to Prof. Georg Schreckenbach who gave me space in his laboratory to use whenever needed, and made me feel like I am part of his research group. Furthermore, I would like to thank Dr. Mansour Almatarneh at the University of Jordan for assisting me in continuing my graduate studies at the University of Manitoba.

I am more than grateful to my parents who supported me and made me feel like a Superman in this world. My dad, Akram, who passed away recently, is one of the crucial reasons that made me want to continue my graduate studies. He supported me in a phenomenal way. Moreover, I extend my love and gratefulness to my mom, Nuha, who made the world trivial to me. Without her, I would not be walking today. I also would like to thank my beloved wife, Oswa, for believing in me and waiting for the many hours, days, and years for me to get things done. I am indeed lucky to have her by my side with her continuous support.

I thank my wonderful sister, Riham, from the bottom of my heart, she is a remarkable gift. As for my brother, Elayan, thank you for inspiring me, and making a positive impact on my way of thinking and taking actions not only in life but also approaching science. I am happy for having this magnificent family by my side.

# Chapter 1

## Introduction

Today, theoretical and computational chemistry has become one of the main sources to understand chemistry, biology, and physics. Computational chemistry is the application of developed theoretical methods, which are based on the laws of physics and mathematics, to predict properties, reaction pathways and energies of various systems. The development of commercial electronic structure packages has made computational chemistry easy to use; thus, scientists from different fields started using it in their research, where simulations now complement theory and experiment to approach science with enhanced accuracy.

Through the years, crucial insights were provided via computational chemistry in catalytic processes, reaction mechanisms, drug design and delivery, as well as other challenges in science.<sup>1,2</sup> However, there is one crucial factor that leads to method development: accuracy and speed. Computational benchmarks prove that the development process is still required to achieve closer accuracy to experimental results and mitigate the different challenges. These challenges include but not limited to predicting: reaction energy barriers and electron correlation.

The applications of quantum mechanics (computational chemistry) have been growing rapidly with an unparalleled impact to science. Hartree–Fock (HF) theory was able to describe molecular geometries.<sup>3</sup> Moreover, systems were properly described with density functional theory (DFT) with lower computational cost and inclusion of electron correlation.<sup>4</sup>

On the other hand, post-HF methods that are more accurate than both the former and the latter theories, became the source of data comparable to experiment. However, with that accuracy, the computational cost is daunting.

The aim of this thesis is to provide insights on the description of electron correlation in small systems such as hydrogen clusters. Providing insights shall be described by our developed method,  $\Delta$ NO. It is not just the idea to illustrate the energy in straight chain systems by stretching them, but to distort molecular geometries as well, and therefore understand how the  $\Delta$ NO method performs.

This work describes the computational tests of the method over challenges that dominate conventional methods; HF, DFT, and post-HF. The first chapter of the thesis is a brief theoretical introduction. The second is a submitted chapter to the Journal of Chemical Theory and Computation that includes derivation of the  $\Delta$ NO method and the systems used to test it. It should be noted, however, that deriving the mathematical equations is not a purpose of this thesis, rather brief summary of them whenever necessary, as these are found in any quantum chemistry book. The thesis is finalized by a summary and future research chapter.

## 1.1 Theoretical Background

### 1.1.1 The Schrödinger Equation

Since the birth of quantum chemistry, the main dilemma was and still is solving the Schrödinger equation. The time-independent, non-relativistic, Schrödinger equation is,

$$\hat{H}\Psi = E\Psi \tag{1.1}$$

where the molecular Hamiltonian,  $\hat{H}$ , operates on the wave function of the system, *e.g.* atom or molecule,  $\Psi$ , and returns an eigenvalue, which is the energy,  $E$ . All equations defined in this thesis are given in atomic units.<sup>3</sup> In  $\hat{H}$ , there are five components of the total energy of

the system,

$$\hat{H} = -\frac{1}{2} \sum_{i=1}^N \nabla_i^2 - \frac{1}{2} \sum_{A=1}^M \frac{1}{M_A} \nabla_A^2 - \sum_{i=1}^N \sum_{A=1}^M \frac{Z_A}{r_{iA}} + \sum_{i=1}^N \sum_{j>i}^N \frac{1}{r_{ij}} + \sum_{A=1}^M \sum_{B>A}^M \frac{Z_A Z_B}{R_{AB}} \quad (1.2)$$

The Laplacian operators,  $\nabla_i^2$  and  $\nabla_A^2$ , are the second derivative with respect to coordinates of electron  $i$  and nucleus  $A$ , respectively. The mass ratio,  $M_A$ , is of nucleus  $A$  to the mass of an electron, and  $Z$  is the atomic number of the nucleus. The distance between electrons and nuclei is;  $r_{iA} = |\mathbf{r}_i - \mathbf{R}_A|$ , whereas distance between electrons is;  $r_{ij} = |\mathbf{r}_i - \mathbf{r}_j|$ , while distance between nuclei is;  $R_{AB} = |\mathbf{R}_A - \mathbf{R}_B|$ . The first and second terms are the kinetic energies of the electrons and nuclei, respectively. The third energy term represents the interaction between electrons and nuclei. The final two terms are the electron–electron Coulomb and nuclei-nuclei interactions.

### 1.1.2 The Variation Principle

In order to evaluate the performance of developed methods, it is critical to account for the variational theorem and check whether the energy is variational or not. In general, the energy is evaluated by taking the expectation value of  $\hat{H}$  for a given trial wave function, which leads to the ground state energy,  $E$ , of the trial wave function. For a wave function,  $\Psi_o$ , the energy can be evaluated as,

$$\frac{\langle \Psi_o | \hat{H} | \Psi_o \rangle}{\langle \Psi_o | \Psi_o \rangle} = E_o \quad (1.3)$$

Assuming there is an approximate wave function,  $\psi$ , that is normalized and well-behaved within the boundary conditions leads to,

$$\langle \psi | \psi \rangle = 1 \quad (1.4)$$

then taking the expectation value of  $\hat{H}$  results in an energy that is an upper bound to  $E_o$ ,

$$\langle \psi | \hat{H} | \psi \rangle = E \geq E_o \quad (1.5)$$

For a ground state system, the variational principle states that the approximate energy is always higher than the exact ground state energy. The equality, however, holds when  $|\psi\rangle = |\Psi_o\rangle$ . Therefore, it is possible to evaluate the quality of the wave function based on its calculated energy, where generally the lower it is, the better the wave function.

### 1.1.3 The Born–Oppenheimer Approximation

The Born–Oppenheimer approximation is based on the fact that the mass of nuclei is much larger than the mass of electrons, and therefore, from an electronic perspective, electrons in a molecule tend to move fast while nuclei remain fixed. The consequences of this is that the molecular wave function is factored into nuclear and electronic wave functions,  $\Psi_{\text{mol}} = \Psi_{\text{nuc}}\Psi_{\text{elec}}$ . This leads to two separate equations: one for the electronic motion and the other is for the nuclear motion. The Hamiltonian of the electronic Schrödinger equation is given by,

$$\hat{H}_{\text{elec}} = -\frac{1}{2} \sum_{i=1}^N \nabla_i^2 - \sum_{i=1}^N \sum_{A=1}^M \frac{Z_A}{r_{iA}} + \sum_{i=1}^N \sum_{j>i}^N \frac{1}{r_{ij}} \quad (1.6)$$

The electronic wave function,  $\Psi_{\text{elec}}(\{\mathbf{r}_i\}; \{\mathbf{R}_A\})$ , is dependent on the electronic coordinates. Furthermore, it also parametrically depends on the nuclear coordinates, where different orientations of the nuclei results in a different function  $\Psi_{\text{elec}}$ . The nuclear coordinates, however, do not appear explicitly in  $\Psi_{\text{elec}}$ . The parametric dependence is also present in the electronic energy,  $E_{\text{elec}} = E_{\text{elec}}(\{\mathbf{r}_i\}; \{\mathbf{R}_A\})$ . The electronic Schrödinger equation is,

$$\hat{H}_{\text{elec}}\Psi_{\text{elec}} = E_{\text{elec}}\Psi_{\text{elec}} \quad (1.7)$$

where the molecular potential energy,  $U$ , is defined as,

$$U = E_{\text{elec}} + \sum_{A=1}^M \sum_{B>A}^M \frac{Z_A Z_B}{R_{AB}} \quad (1.8)$$

The problem of Equation 1.7 is the presence of the Coulomb repulsion term that makes finding an exact solution to the equation unattainable for  $N > 1$ . The subscript *elec* drops

from the equations as the Hamiltonians and wave functions that follow are considered are electronic.

### 1.1.4 Hartree–Fock Theory

The HF is a simple approximation for a wave function describing a system of  $N$  electrons. It approximates the wave function by a single Slater determinant (Equation 1.9), which satisfies the antisymmetry of the electronic wave function, *i.e.*, Pauli exclusion principle. The antisymmetry ensures that the sign of the wave function changes due to the interchange of two of the electronic coordinates,  $\Psi(\mathbf{x}_1, \mathbf{x}_2) = -\Psi(\mathbf{x}_2, \mathbf{x}_1)$ . A Slater determinant is written as,

$$\Psi(\mathbf{x}_1, \mathbf{x}_2, \dots, \mathbf{x}_N) = \frac{1}{\sqrt{N!}} \begin{vmatrix} \chi_i(\mathbf{x}_1) & \chi_j(\mathbf{x}_1) & \cdots & \chi_k(\mathbf{x}_1) \\ \chi_i(\mathbf{x}_2) & \chi_j(\mathbf{x}_2) & \cdots & \chi_k(\mathbf{x}_2) \\ \vdots & \vdots & & \vdots \\ \chi_i(\mathbf{x}_N) & \chi_j(\mathbf{x}_N) & \cdots & \chi_k(\mathbf{x}_N) \end{vmatrix} \quad (1.9)$$

where  $\frac{1}{\sqrt{N!}}$  is a normalization factor, and the spin orbitals  $\chi$  are functions of the spatial and spin electronic coordinates,  $\mathbf{x} = (\mathbf{r}, \omega)$ . Each spatial orbital,  $\psi(\mathbf{r})$ , can form two spin orbitals with different spin functions,  $\alpha(\omega)$  or  $\beta(\omega)$ , by taking their product

$$\chi = \begin{cases} \psi(\mathbf{r})\alpha(\omega) \\ \text{or} \\ \psi(\mathbf{r})\beta(\omega) \end{cases} \quad (1.10)$$

Slater determinants meet the antisymmetry requirement, and thus, the electrons of the wave function are indistinguishable.

The HF energy is given by the expectation value of  $\hat{H}$ , and the HF wave function,  $\Psi_{HF}$ ,

$$\begin{aligned} \langle \Psi_{HF} | \hat{H} | \Psi_{HF} \rangle &= E_{HF} \\ &= \sum_{i=1}^N h_{ii} + \frac{1}{2} \sum_{i=1}^N \sum_{j=1}^N J_{ij} - K_{ij} \end{aligned} \quad (1.11)$$

where the first term is the one-electron energy term,

$$h_{ii} = \int \chi_i^*(\mathbf{x}_1) \left( -\frac{1}{2} \nabla_i^2 - \sum_A \frac{Z_A}{r_{iA}} \right) \chi_i(\mathbf{x}_1) d\mathbf{x}_1 \quad (1.12)$$

and the two-electron part consists of the Coulomb and exchange interactions,  $J_{ij}$  and  $K_{ij}$ , respectively.

$$J_{ij} = \iint \chi_i^*(\mathbf{x}_1) \chi_i(\mathbf{x}_1) \frac{1}{r_{12}} \chi_j^*(\mathbf{x}_2) \chi_j(\mathbf{x}_2) d\mathbf{x}_1 d\mathbf{x}_2 \quad (1.13a)$$

$$K_{ij} = \iint \chi_i^*(\mathbf{x}_1) \chi_j(\mathbf{x}_1) \frac{1}{r_{12}} \chi_j^*(\mathbf{x}_2) \chi_i(\mathbf{x}_2) d\mathbf{x}_1 d\mathbf{x}_2 \quad (1.13b)$$

The HF equations can also be written in terms of the spatial orbitals,  $\psi(\mathbf{r})$ , by expanding and integrating over the spin from the integrals. The HF energy is expressed as,

$$E_{HF} = 2 \sum_{a=1}^{N/2} h_{aa} + \sum_{a=1}^{N/2} \sum_{b=1}^{N/2} 2J_{ab} - K_{ab} \quad (1.14)$$

The energy expression is based on the double occupation of the molecular orbitals (MOs), *i.e.*, a closed-shell system. The one electron-energy,  $h_{aa}$ , and two-electron energy terms,  $J_{ab}$  and  $K_{ab}$ , are defined in terms of the spatial orbital,  $\psi(\mathbf{r})$ .

Minimizing the energy (Equation 1.11) with respect to the orthonormal spin orbitals derives the HF equations.

$$\hat{f}(\mathbf{r}_1) \psi_i(\mathbf{r}_1) = \epsilon_i \psi_i(\mathbf{r}_1) \quad (1.15)$$

where  $\epsilon_i$  is the orbital energy and  $\hat{f}$  is the Fock operator, which is expressed as,

$$\hat{f}(\mathbf{r}_1) = \hat{h}(\mathbf{r}_1) + \sum_{a=1}^{N/2} 2\hat{J}_a(\mathbf{r}_1) - \hat{K}_a(\mathbf{r}_1) \quad (1.16)$$

where,

$$\hat{h} = -\frac{1}{2}\nabla_1^2 - \sum_A \frac{Z_A}{r_{1A}} \quad (1.17a)$$

$$\hat{J}_a(\mathbf{r}_1) = \int \psi_a^*(\mathbf{r}_2) \frac{1}{r_{12}} \psi_a(\mathbf{r}_2) d\mathbf{r}_2 \quad (1.17b)$$

$$\hat{K}_a(\mathbf{r}_1) = \int \psi_a^*(\mathbf{r}_2) \frac{1}{r_{12}} \hat{P}_{12} \psi_a(\mathbf{r}_2) d\mathbf{r}_2 \quad (1.17c)$$

and  $\hat{P}_{12}$  is a permutation operator of electron labels.

In order to obtain a solution for the HF equations, Roothaan–Hall equations provide a simple approach by introducing a set of known  $K$  basis functions, and expanding the unknown MOs as a linear combination of basis functions,  $\phi(\mathbf{r})$ ,

$$\psi_i = \sum_{\nu=1}^K C_{\nu i} \phi_{\nu}(\mathbf{r}_1) \quad (1.18)$$

The linear expansion is substituted into the HF equation (Equation 1.15), and both sides of the equation are multiplied by the basis function complex conjugate,  $\phi_{\mu}^*(\mathbf{r}_1)$ , and integrated,

$$\sum_{\nu} C_{\nu i} \int \phi_{\mu}^*(\mathbf{r}_1) \hat{f}(\mathbf{r}_1) \phi_{\nu}(\mathbf{r}_1) d\mathbf{r}_1 = \epsilon_i \sum_{\nu} C_{\nu i} \int \phi_{\mu}^*(\mathbf{r}_1) \phi_{\nu}(\mathbf{r}_1) d\mathbf{r}_1 \quad (1.19)$$

This is a matrix equation recognized as Roothaan–Hall equation, where its integrated form can be expressed in a compact matrix equation as,

$$\mathbf{FC} = \mathbf{SC}\epsilon \quad (1.20)$$

where  $\mathbf{C}$  is a  $K \times K$  square matrix that represents the MO coefficients. Elements of the Fock matrix are given by,

$$F_{\mu\nu} = \int \phi_{\mu}^*(\mathbf{r}_1) \hat{f}(\mathbf{r}_1) \phi_{\nu}(\mathbf{r}_1) d\mathbf{r}_1 \quad (1.21)$$

the overlap matrix is,

$$S_{\mu\nu} = \int \phi_{\mu}^*(\mathbf{r}_1) \phi_{\nu}(\mathbf{r}_1) d\mathbf{r}_1 \quad (1.22)$$

and  $\epsilon$  is a diagonal matrix of the orbital energies. The approach of solving Roothaan's equation is known as self-consistent field (SCF) procedure, which is an iterative way to solve the equation. It is initialized by a guess of the coefficient matrix and finalized by the convergence of the energy or coefficients. However, the main drawback of the HF wave function method is the neglected part of electron interactions, which can lead to rather incorrect energy values.

### 1.1.5 Electron Correlation

The HF method approximates the wave function as a single Slater determinant, and thus, it describes the exchange interaction between parallel spin electrons properly. HF treats electron interactions at an average mean-field level, where each electron experiences the generated field of other electrons. It does not correlate the interaction between parallel and anti-parallel spin electrons, which is known as Coulomb correlation. Thus, HF is considered useless in dealing with properties that are strongly influenced by electron correlation, *e.g.*, dipole moments.

The difference between the HF energy from the exact energy value is recognized as the electron correlation energy,  $E_c$ .<sup>1,3</sup>

$$E_c = E_{\text{exact}} - E_{\text{HF}} \quad (1.23)$$

The exact energy,  $E_{\text{exact}}$ , is the non-relativistic energy, of the system and  $E_{\text{HF}}$  is the HF energy, within a complete limit of the basis set.  $E_c$  corresponds to a small fraction of the total electronic energy.<sup>5</sup> However, it is vital for calculating accurate reaction energies, bond lengths, band gaps, and other properties.<sup>6</sup> Furthermore, for a more convenient understanding of  $E_c$ , it is sometimes partitioned into two parts; static correlation energy,  $E_{\text{stat}}$ , and dynamic correlation energy,  $E_{\text{dyn}}$ .<sup>7-9</sup>

$$E_c = E_{\text{stat}} + E_{\text{dyn}} \quad (1.24)$$

Static correlation, occurs when different electronic configurations, *i.e.*, Slater determinants have exact or near-degeneracy with the HF ground state configuration.<sup>1,10</sup> It is also referred to as near-degeneracy, nondynamic, and strong correlation.<sup>11–14</sup> The main flaw is the single Slater determinant, and if a multireference approach is utilized, then  $E_{\text{stat}}$  would be properly included. Dynamic correlation, however, is critical for the relative motion of electrons. There are two parts of  $E_{\text{dyn}}$ ; the first is short-range,  $E_{\text{sr-dyn}}$ ,<sup>15</sup> and describes the electron–electron cusp; the second is long-range,  $E_{\text{lr-dyn}}$ ,<sup>16</sup> which is necessary for describing van der Waals interactions, which are referred to as dispersion,

$$E_{\text{dyn}} = E_{\text{sr-dyn}} + E_{\text{lr-dyn}} \tag{1.25}$$

There is no magical method or approach to use for all physical-chemical systems; however, it is possible to provide one that is more accurate and efficient than current methods.

### 1.1.6 Density Functional Theory

The foundation for density functional theory (DFT) is set by the Hohenberg and Kohn<sup>17</sup> theorems where the ground state electronic energy of a system is defined as a functional of the total electron density,  $\rho(\mathbf{r})$ .

$$E = E[\rho(\mathbf{r})] \tag{1.26}$$

The Hohenberg–Kohn theorem states that for a system with an external potential,  $\nu_{\text{ext}}$ , there is a uniquely determined ground state wave function,  $\Psi_o$ , as well as a unique one-electron density,  $\rho_o(\mathbf{r})$ .<sup>17</sup> Thus, the ground state energy,  $E_o$ , is also determined. Furthermore, in order to obtain a variational functional,  $E[\rho(\mathbf{r})] \geq E_o$ , certain constraints must be followed, that include the non-negative condition on the electron density and integrating to the total number of electrons in a system,

$$\rho(\mathbf{r}) \geq 0 \quad (1.27a)$$

$$\int \rho(\mathbf{r}) d\mathbf{r} = N \quad (1.27b)$$

The ground state energy of a non-degenerate system is expressed with two terms; the external potential,  $\nu_{\text{ext}}[\rho(\mathbf{r})]$ , and the universal functional,  $F[\rho(\mathbf{r})]$ .

$$E[\rho(\mathbf{r})] = \nu_{\text{ext}}[\rho(\mathbf{r})] + F[\rho(\mathbf{r})] \quad (1.28)$$

The lack of an applied field leads to the potential provided by the nuclei,  $V_{ne}[\rho(\mathbf{r})]$ ,

$$\nu_{\text{ext}}[\rho(\mathbf{r})] = V_{ne}[\rho(\mathbf{r})] = - \sum_{A=1}^M \int \frac{Z_A}{r_{1A}} \rho(\mathbf{r}) d\mathbf{r}_1 \quad (1.29)$$

The  $F[\rho(\mathbf{r})]$  term, which is independent of the external field, is a density functional that includes both the total kinetic energy and Coulomb repulsion energy of the electrons.

$$F[\rho(\mathbf{r})] = T[\rho(\mathbf{r})] + V_{ee}[\rho(\mathbf{r})] \quad (1.30)$$

Both terms included in  $F[\rho(\mathbf{r})]$  exist, however, there is no known explicit form for them and thus,  $F[\rho(\mathbf{r})]$  is an unknown functional. In order to tackle this issue, both terms in  $F[\rho(\mathbf{r})]$  are approximated. The Kohn–Sham approach utilizes a system of non-interacting electrons by using Kohn–Sham orbitals,  $\chi_i^{KS}(\mathbf{r})$ , where the Kohn–Sham electron density,  $\rho^{KS}(\mathbf{r})$ , is equivalent to the ground state electron density,  $\rho_o(\mathbf{r})$ . Consider a single Slater determinant (Equation 1.9) of orthonormal  $\chi_i^{KS}$ ,

$$\rho^{KS}(\mathbf{r}) = \sum_{i=1}^N |\chi_i^{KS}(\mathbf{r})|^2 \quad (1.31)$$

and total kinetic energy of,

$$T_s[\rho(\mathbf{r})] = -\frac{1}{2} \sum_{i=1}^N \langle \chi_i^{KS}(\mathbf{r}_1) | \nabla_1^2 | \chi_i^{KS}(\mathbf{r}_1) \rangle \quad (1.32)$$

The second term of Equation (1.30) is approximated using the classical Coulomb energy term,

$$J[\rho(\mathbf{r})] = \frac{1}{2} \iint \frac{\rho(\mathbf{r}_1)\rho(\mathbf{r}_2)}{r_{12}} d\mathbf{r}_1 d\mathbf{r}_2 \quad (1.33)$$

The errors made by these approximations of both terms are recognized in the exchange-correlation energy functional,  $E_{xc}$ , which has an unknown explicit form. Thus, Equation (1.30) can be re-expressed as,

$$F[\rho(\mathbf{r})] = T_s[\rho(\mathbf{r})] + J[\rho(\mathbf{r})] + E_{xc}[\rho(\mathbf{r})] \quad (1.34)$$

The  $E_{xc}[\rho(\mathbf{r})]$  includes a correction to the kinetic energy due to the interaction of electrons in a non-interacting system,  $\Delta T[\rho(\mathbf{r})]$ , the self-interaction correction present in the Coulomb energy term, *e.g.*,  $J[\rho(\mathbf{r})] > 0$  for a one-electron system, Equation (1.33), and the electron-electron exchange as well as correlation effects,  $\Delta V_{ee}[\rho(\mathbf{r})]$ .

$$\begin{aligned} E_{xc}[\rho(\mathbf{r})] &= (T[\rho(\mathbf{r})] - T_s[\rho(\mathbf{r})]) + (V_{ee}[\rho(\mathbf{r})] - J[\rho(\mathbf{r})]) \\ &= \Delta T[\rho(\mathbf{r})] + \Delta V_{ee}[\rho(\mathbf{r})] \end{aligned} \quad (1.35)$$

Substituting Equations 1.29 and 1.34 into Equation (1.28), formulates the Kohn–Sham energy functional,

$$E[\rho(\mathbf{r})] = T_s[\rho(\mathbf{r})] + V_{ne}[\rho(\mathbf{r})] + J[\rho(\mathbf{r})] + E_{xc}[\rho(\mathbf{r})] \quad (1.36)$$

The significance of this energy expression is that there are two exact terms,  $T_s[\rho(\mathbf{r})]$  and  $V_{ne}[\rho(\mathbf{r})]$ , while the final term,  $E_{xc}[\rho(\mathbf{r})]$ , constitutes a small part of the total energy. The energy expression,  $E[\rho(\mathbf{r})]$ , is minimized with respect to  $\chi_i^{KS}(\mathbf{r})$ , which yields the Kohn–Sham orbital equation.

$$\hat{f}_i^{KS}(\mathbf{r}_1)\chi_i^{KS}(\mathbf{r}_1) = \epsilon_i\chi_i^{KS}(\mathbf{r}_1) \quad (1.37)$$

where  $\hat{f}_i^{KS}(\mathbf{r}_1)$  is the Kohn–Sham one-electron operator.

$$\hat{f}_i^{KS}(\mathbf{r}_1) = -\frac{1}{2}\nabla_1^2 - \sum_{A=1}^M \frac{Z_A}{r_{1A}} + \int \frac{\rho(\mathbf{r}_2)}{r_{12}} d\mathbf{r}_2 + \frac{\delta E_{xc}[\rho(\mathbf{r})]}{\delta \rho(\mathbf{r})} \quad (1.38)$$

The final term,  $\frac{\delta E_{xc}[\rho(\mathbf{r})]}{\delta \rho(\mathbf{r})}$ , is the functional derivative of  $E_{xc}$  with respect to  $\rho(\mathbf{r})$ . Furthermore, the approach of minimizing the energy in Equation 1.37 is similar to the HF Equation (1.15). It also depends on the electron density, and the equations are solved similar to HF, using an SCF approach, iteratively.

The simplicity in DFT is not restricted to its mathematical equations, but also to its computational cost. Hybrid methods are comparable to HF, while pure methods are lower in cost than HF. DFT is known as an exact theory, where the solution to the Kohn–Sham equations give the exact ground state energy. However, due to the approximations made to the unknown exchange-correlation energy term, the solutions provided and their energies are approximate. Furthermore, these approximations excludes DFT from being variational.

Density functional approximations are known to accurately account for  $E_{\text{sr-dyn}}$  term (Equation 1.25). Although part of  $E_{\text{dyn}}$  is properly described, the other part,  $E_{\text{lr-dyn}}$ , represents another challenge to DFT. Each density functional approximation has its own accuracy and limitation, depending on the system and the addressed questions. However, static correlation remains a significant challenge to the theory. This is due to the fact that DFT, like HF, utilizes a single Slater determinant, while in order to describe  $E_{\text{stat}}$ , a multireference approach must be devised.

### 1.1.7 Post Hartree–Fock Methods

Post–HF methods use the ground state HF Slater determinant as their basis. In configuration interaction (CI), the wave function is considered as a linear combination of Slater determinants with excitations from the occupied  $(a, b, c)$  to virtual  $(r, s, t)$  spin orbitals.

$$\Phi_o = c_o \Psi_o + \sum_{ar} c_a^r \Psi_a^r + \sum_{\substack{a<b \\ r<s}} c_{ab}^{rs} \Psi_{ab}^{rs} + \sum_{\substack{a<b<c \\ r<s<t}} c_{abc}^{rst} \Psi_{abc}^{rst} + \dots \quad (1.39)$$

The possible excitations are based on the HF wave function,  $\Psi_o$ , where they include but are not limited to single,  $\Psi_a^r$ , double,  $\Psi_{ab}^{rs}$ , and triple excitations,  $\Psi_{abc}^{rst}$ , multiplied by their expansion coefficients,  $c_a^r$ ,  $c_{ab}^{rs}$ , etc. This constitutes the theory known as configuration interaction (CI). The CI coefficients are found via the variation principle, and CI is variational because Slater determinants are well-behaved and it is a linear combination. Once all possible configurations in a given system are included in  $\Phi_o$  (Equation 1.39), in the limit of a complete basis set, the exact non-relativistic energy is reached, this is referred to as full CI.

Although it is possible to consider full CI, it is not feasible for use in large systems and restricts its application to small ones, depending on the basis sets used. This is due to the extensive computational resources required, where the cost is exponential with respect to the number of basis functions. It is possible, however, to truncate the expansion to a limited order or type of excitation, single (CIS), double (CISD), triple (CISDT), *etc.* The main drawback of truncated CI wave functions is that they are no longer size-consistent.

Size-consistency is vital in chemistry, where a method is considered size-consistent when the energy of non-interacting molecules (monomers) is equal to the sum of their individual energies. For example, consider two non-interacting hydrogen molecules ( $\text{H}_2 \cdots \text{H}_2$ ); the total calculated energy is twice that calculated for the individual molecules,

$$E_{(\text{H}_2-\text{H}_2)} = 2E_{(\text{H}_2)} \tag{1.40}$$

The relative energy,  $\Delta E$ , of this system at  $R = \infty$  is exactly zero. Among the methods that are size consistent are full CI, HF, Møller–Plesset ( $\text{MP}_n$ ), and coupled-cluster (CC) theories.

The wave function in CC theory,  $\Psi_{\text{CC}}$ , is expressed as a cluster of a ground state HF reference wave function,

$$\Psi_{\text{CC}} = e^{\hat{T}} \Psi_o \tag{1.41}$$

where the exponential ansatz,  $e^{\hat{T}}$ , results in products of excitations included directly in the

wave function.

$$e^{\hat{T}} = 1 + \hat{T} + \frac{\hat{T}^2}{2!} + \frac{\hat{T}^3}{3!} + \dots \quad (1.42)$$

The excitation operator,  $\hat{T}$ , is responsible for the operators acting on the HF wave function,  $|\Psi_o\rangle$ . The sum of various operators (Equation 1.41) are included in  $\hat{T}$ ,

$$\hat{T} = \sum_{i=1}^N \hat{T}_i \quad (1.43)$$

Thus, it excites electrons from the occupied to virtual spin orbitals. For example, the singles excitation operator,  $\hat{T}_1$ , acting on the HF wave function is expressed as,

$$\hat{T}_1 \Psi_o = \sum_{ar} c_a^r \Psi_a^r \quad (1.44)$$

The excitations could be singles, doubles, triples, or quadruples, etc. Hence, the method is defined by which excitation operators are included; CCS, CCSD, CCSDT, or CCSDTQ. The most well-known CC method is CCSD(T), where the triple excitations are calculated using perturbation theory. The advantage of using CC theory is its accuracy in computing energy values, and it is also size consistent. However, the computational cost limits their use to some degree, which depends on the system and basis functions. For example, the computational cost of CCSD(T) scales as  $K^7$ , where  $K$  is the number of basis functions, which makes it rather expensive for molecules with more than 12 heavy atoms, which are atoms other than hydrogen. Furthermore, although CC methods are size-consistent, which is due to the presence of  $e^{\hat{T}}$ , they are not variational. The calculated energy could be lower than the exact, non-relativistic, energy.

Another post-HF method is Møller–Plesset perturbation theory, where the exact Hamiltonian,  $\hat{H}$ , is partitioned into the unperturbed HF Hamiltonian operator,  $\hat{H}_0$ , and the perturbation operator,  $\hat{V}$ .

$$\hat{H} = \hat{H}_0 + \lambda \hat{V} \quad (1.45)$$

where

$$\hat{H}_0 = \sum_i \hat{f}_i \quad (1.46)$$

and  $\hat{V}$  is a correction term and defined as,

$$\hat{V} = \sum_{i=1}^N \sum_{j>i}^N \frac{1}{r_{ij}} - \sum_{i=1}^N \sum_{j=1}^N [\hat{J}_j(i) - \hat{K}_j(i)] \quad (1.47)$$

The ordering parameter,  $\lambda$ , determines the strength of perturbation. The energy can be written as an expansion of energy corrections,  $E^n$ , where the total energy is the sum of the these energy parts,

$$E = E^0 + E^1 + E^2 + \dots \quad (1.48)$$

The first-order energy, the first two terms of Equation (1.48) is given by,

$$\begin{aligned} E_{\text{MP1}} &= E^0 + E^1 \\ &= \langle \Psi | \hat{H}^0 | \Psi \rangle + \langle \Psi | \hat{V}^1 | \Psi \rangle \\ &= \langle \Psi_{\text{HF}} | \hat{H} | \Psi_{\text{HF}} \rangle \end{aligned} \quad (1.49)$$

The first correction,  $\hat{V}$ , of the HF energy leads to actual treatment of  $E_c$ , which is referred to as second-order (MP2), while other higher order corrections are know as third-order (MP3), or fourth-order (MP4) energy. In the spin orbital basis, the energy expression of MP2 is given as,

$$E(\text{MP2}) = \sum_{\substack{i<j \\ a<b}} \frac{|\langle ij || ab \rangle|^2}{\epsilon_i + \epsilon_j - \epsilon_a - \epsilon_b} \quad (1.50)$$

where,

$$\langle ij || ab \rangle = \langle ij | ab \rangle - \langle ij | ba \rangle \quad (1.51a)$$

$$\langle ij | ab \rangle = \iint \psi_i^*(\mathbf{r}_1) \psi_j(\mathbf{r}_1) \frac{1}{r_{12}} \psi_a^*(\mathbf{r}_2) \psi_b(\mathbf{r}_2) d\mathbf{r}_1 d\mathbf{r}_2 \quad (1.51b)$$

## 1.2 Hartree–Fock Dissociation of Molecules

Hartree–Fock theory has different formalisms for treating electrons in a Slater determinant (Equation 1.9); restricted (RHF), restricted open-shell (ROHF), and unrestricted (UHF).<sup>3,18</sup>

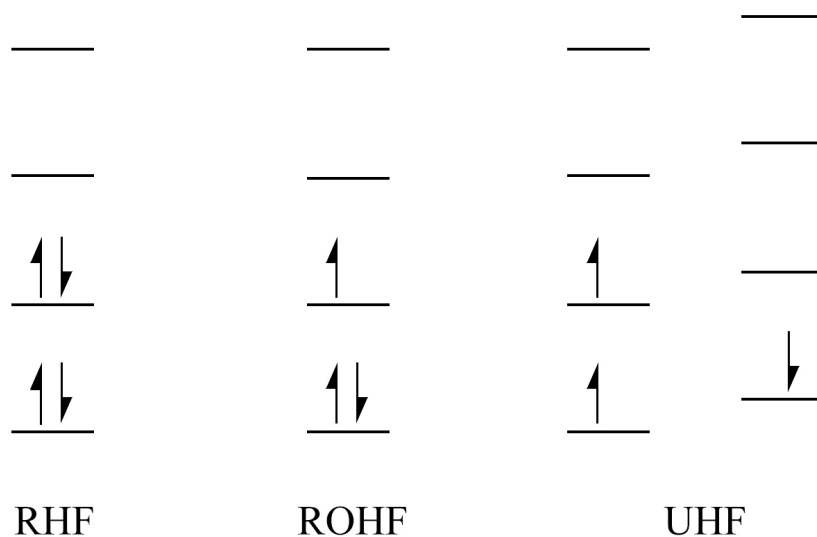


Figure 1.1: Description of an RHF singlet state, ROHF and UHF doublet states. Lines indicate the energy of spatial orbitals.

For a closed-shell singlet system, the RHF constructs the determinant with the restriction that each spatial orbital,  $\psi(\mathbf{r})$ , has two electrons, one with  $\alpha$  and one with  $\beta$  spin. For an open-shell system, it is possible to be described with a restricted type wave functions utilizing ROHF, see Figure 1.1. The more common approach is using UHF, which constructs the determinant where the  $\alpha$  and  $\beta$  spins can have different set of  $\psi(\mathbf{r})$ . However, the spin symmetry breaks, where the UHF wave function is no longer an eigenfunction of the spin operator,  $\hat{S}^2$ , and is said to be spin contaminated. For an unrestricted singlet state, for instance, the wave function contains contributions from higher states, *i.e.*, triplet and quintet multiplicities, that contaminate the wave function. This is also observed for doublet states, where it is contaminated by higher order multiplicity components, *i.e.*, quartet, sextet, etc. Thus, in a spin contaminated wave function, the expectation value of  $\hat{S}^2$  is high for a UHF wave function, compared to the expected value calculated as  $\langle \hat{S}^2 \rangle = S(S + 1)$ .

In terms of the predicted energy, the UHF wave function predicts either lower than or equal energy to ROHF.<sup>19</sup> For singlet systems within reach of the equilibrium region, it is not usually possible to obtain a lower energy using a UHF wave function. However, stretching

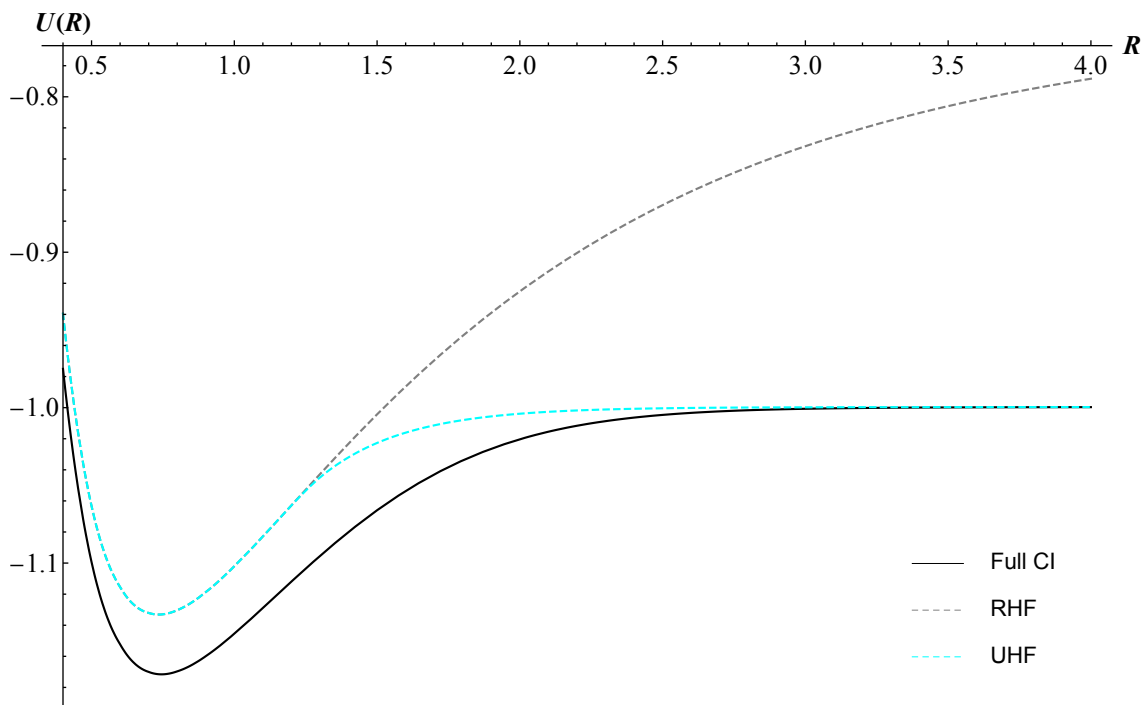


Figure 1.2: Dissociation of  $\text{H}_2$  as a function of bond length. Selected basis set cc-pVTZ.

the bond beyond equilibrium, leads to the breakage of spin symmetry due to the mixing of the lowest triplet state with the singlet ground state. The breaking symmetry point is recognized as the Coulson–Fischer point on the PES.<sup>20</sup>

Considering  $\text{H}_2$ , for example, at dissociation limit it has an equal mixture of covalent,  $\text{H}^-\text{H}^+$ , and ionic,  $\text{H}^+\text{H}^-$ , bonding. For homolytic dissociation, the covalent contribution should be completely dominant, where the dissociation limit has two separate  $\text{H}^\cdot$  radicals. RHF, however, dissociates the bond with a 50% mixture of covalent and ionic contribution at dissociation limit, and thus, the resulting energy is always higher than the UHF energy, see Figure 1.2. This affects not only dissociation energies, but also leads to higher activation energies. Furthermore, the equilibrium bond lengths are most likely shorter than expected. This results in higher calculated vibrational frequencies as well. On the other hand, by breaking the spin symmetry, UHF wave function localizes the electrons on the nucleus. Moreover, UHF partially accounts for  $E_c$ , where it generally increases as the bond is stretched. Compared to full CI at equilibrium ( $R = 0.74 \text{ \AA}$ ), the UHF energy is higher by  $102 \text{ kJ mol}^{-1}$ . As

the spin symmetry breaks at  $R = 1.22 \text{ \AA}$ , UHF energies deviate from RHF until it becomes consistent with full CI energies. At complete dissociation, RHF overestimates the energy by  $555 \text{ kJ mol}^{-1}$ .

# References

- [1] Cramer, C. J. *Essentials of Computational Chemistry: Theories and Models*; John Wiley & Sons Ltd: West Sussex, 2004.
- [2] Vogiatzis, K. D.; Polynski, M. V.; Kirkland, J. K.; Townsend, J.; Hashemi, A.; Liu, C.; Pidko, E. A. Computational Approach to Molecular Catalysis by 3d Transition Metals: Challenges and Opportunities. *Chemical Reviews* **2019**, *119*, 2453–2523.
- [3] Szabo, A.; Ostlund, N. S. *Modern quantum chemistry*; Dover: New York, 1996.
- [4] Cohen, J. A.; Mori-Sánchez, P.; Yang, W. Challenges for Density Functional Theory. *Chem. Rev.* **2012**, *112*, 289–320.
- [5] Levine, I. N. *Quantum Chemistry*; Pearson: New Jersey, 2014.
- [6] Foulkes, W. M. C.; Mitas, L.; Needs, R. J.; Rajagopal, G. Quantum Monte Carlo simulations of solids. *Rev. Mod. Phys.* **2001**, *73*, 33–83.
- [7] Mok, D. K. W.; Neumann, R.; Handy, N. C. Dynamical and Nondynamical Correlation. *J. Phys. Chem.* **1996**, *100*, 6225–6230.
- [8] Handy, N. C.; Cohen, A. J. Left-right correlation energy. *Mol. Phys.* **2001**, *99*, 403–412.
- [9] Tsuchimochi, T.; Voorhis, T. V. Extended Møller-Plesset perturbation theory for dynamical and static correlations. *J. Chem. Phys.* **2014**, *141*, 164117.
- [10] Helgaker, T.; Jorgensen, P.; Olsen, J. *Molecular Electronic-Structure Theory*; John Wiley & Sons Ltd: New York, 2013.

- [11] Molawi, K.; Cohen, A. J.; Handy, N. C. Left–right and dynamic correlation. *Int. J. Quantum Chem.* **2002**, *89*, 86–93.
- [12] Hollett, J. W.; Gill, P. M. W. The two faces of static correlation. *J. Chem. Phys.* **2011**, *134*, 114111.
- [13] Becke, A. D. Density functionals for static, dynamical, and strong correlation. *J. Chem. Phys.* **2013**, *138*, 074109.
- [14] Phillips, J. J.; Zgid, D. The description of strong correlation within self-consistent Green’s function second-order perturbation theory. *J. Chem. Phys.* **2014**, *140*, 241101–241107.
- [15] Borden, W.; Davidson, E. The Importance of Including Dynamic Electron Correlation in ab Initio Calculations. *Acc. Chem. Res.* **1996**, *29*, 67.
- [16] London, F. *Z. Physik. Chem. B* **1930**, *11*, 222–251.
- [17] Hohenberg, P.; Kohn, W. Inhomogeneous electron gas. *Phys. Rev.* **1964**, *136*, B864.
- [18] Jensen, F. *Introduction to Computational Chemistry*; John Wiley & Sons Ltd: West Sussex, 2007.
- [19] Mori-Sánchez, J. A., Paula Cohen Qualitative breakdown of the unrestricted Hartree-Fock energy. *J. Chem. Phys.* **2014**, *141*, 164124.
- [20] Coulson, C. A.; Fischer, I. XXXIV. Notes on the molecular orbital treatment of the hydrogen molecule. *The London, Edinburgh, and Dublin Philosophical Magazine and Journal of Science* **1949**, *40*, 386–393.

# Chapter 2

## Performance of $\Delta$ NO Towards Statically Correlated Hydrogen Clusters

### 2.1 Introduction

The proper description of electron correlation remains a dominant challenge in quantum chemistry.<sup>1-3</sup> Density functional theory (DFT) became the common approach due to the computational cost and inclusion of electron correlation energy ( $E_c$ ), which is absent in Hartree–Fock (HF).<sup>4,5</sup> Both methods perform well in systems well-described by a single determinant,<sup>6</sup> however, they encounter difficulties in describing systems with severe static correlation, *i.e.*, multireference character.<sup>7</sup> Hydrogen clusters ( $H_n$  where  $n = 3\dots 50$ ) are well-known statically correlated systems, where molecular orbitals become degenerate upon dissociation.<sup>7-14</sup> They are a prototype for metal-to-insulator transition.<sup>15,16</sup>

The correlation energy ( $E_c$ ) of a chemical system is defined as the difference between the exact non-relativistic energy ( $E_{\text{exact}}$ ) and the HF ground state energy ( $E_{\text{HF}}$ ) in the limit of a complete basis set,<sup>17</sup>

$$E_c = E_{\text{exact}} - E_{\text{HF}} \quad (2.1)$$

where it can be partitioned into two forms of correlation energy, static ( $E_{\text{stat}}$ ) and dynamic ( $E_{\text{dyn}}$ ),<sup>18–24</sup>

$$E_c = E_{\text{stat}} + E_{\text{dyn}} \quad (2.2)$$

Static correlation (also known as near-degeneracy, nondynamic, left-right, or strong correlation)<sup>25–29</sup> results from the near- or exact-degeneracy of the electron configurations with the HF configuration.<sup>30,31</sup> Description of static correlation is required in systems of multireference character, *i.e.*, dissociating molecules,<sup>32–35</sup> radicals,<sup>36–39</sup> transition metal complexes,<sup>40–43</sup> and excited states.<sup>44–47</sup> Dynamic correlation, is the relative motion of electrons through space. It can be decomposed into two components; short-range,<sup>48,49</sup> which is required to describe the electron–electron cusp, and long-range, which is required for dispersion interactions,<sup>50</sup>

$$E_{\text{dyn}} = E_{\text{sr-dyn}} + E_{\text{lr-dyn}} \quad (2.3)$$

Unrestricted Hartree–Fock (UHF)<sup>51</sup> partially accounts for  $E_{\text{stat}}$ ,<sup>31</sup> but the wave function is no longer an eigenfunction of  $\hat{S}^2$ . UHF results in lower energies when spin symmetry is broken. DFT adapts the unrestricted formalism and can partially account for  $E_{\text{stat}}$ .<sup>52,53</sup> Furthermore, it constructs the Slater determinant of Kohn–Sham orbitals and deals quite well with  $E_{\text{sr-dyn}}$ .<sup>54</sup>

A better way to describe systems of multireference character is to construct the wave function as a linear combination of Slater determinants.<sup>55</sup> Multireference self-consistent field (MRSCF) method,<sup>56–59</sup> for example, complete active space self-consistent field (CASSCF),<sup>60–62</sup> mainly accounts for  $E_{\text{stat}}$  and partially for  $E_{\text{dyn}}$ . In order to obtain remaining  $E_{\text{dyn}}$ , post-HF methods are applied to the resulting multireference wave function, such as second-order perturbation theory (PT2)<sup>63–66</sup> and coupled-cluster.<sup>67–70</sup> However, this can lead to double-counting of  $E_{\text{dyn}}$ .<sup>69</sup>

Post-HF methods, such as Møller–Plesset ( $\text{MP}_n$ ,  $n = 2, 3, \dots$ ) perturbation theory, coupled-cluster (CC) theory, deal with  $E_c$  well in some systems, but fail drastically in other systems that are simple in chemistry, *e.g.*, hydrogen clusters.<sup>71–74</sup> Taking all possible excitations of the electrons (determinants) as a linear combination, corresponding to full configuration interaction (full CI), achieves the exact answer.<sup>75,76</sup> The downside of using

these methods is the computational cost, which limits their application to rather simple molecules.<sup>76</sup> Combining post-HF wave functions for  $E_{\text{stat}}$  with density functionals for  $E_{\text{dyn}}$ , faces the same above-mentioned double-counting issue.<sup>77–80</sup>

Recently,<sup>78,81</sup> the advantage of combining MCSCF with an on-top two-electron density functional to deal with static correlation and double counting emerged with multiconfiguration pair-density functional theory (MC-PDFT). The results are promising with lower computational cost than multireference theory, such as MRCI and CASPT2.<sup>81</sup>

Improvements over CC theory,<sup>71,72</sup> restricting to pair excitations in the cluster operator  $\hat{T}$ , (*i.e.* pair coupled cluster doubles),<sup>80</sup> and removing some parts<sup>73</sup> from  $\hat{T}$  to treat static correlation qualitatively treated the failure of traditional CC in stretching hydrogen clusters. However, these CC treatments improve aspects, but leave out other parts of  $E_{\text{stat}}$ .<sup>71–73</sup>

A promising alternative approach in capturing both static and dynamic correlation energies are cumulant functional methods, which include density-matrix functional theory (DMFT)<sup>38</sup> and natural orbital functional theory (NOFT).<sup>82</sup> DMFT is useful in reducing the computational cost compared to wave function methods.<sup>83</sup> NOFT has shown signs of future success in some systems.<sup>84–86</sup> Among the NOFT methods is Piris natural orbital functional (PNOF) that captures static correlation in different systems.<sup>13,15,84,87</sup>

The  $\Delta\text{NO}$ <sup>85</sup> method, which is based on cumulant functional theory (CFT), combines an effective cumulant functional for static correlation with an on-top two-electron density functional,<sup>88,89</sup> or more recently with post-HF functionals,<sup>90</sup> for short-range dynamic correlation. Unlike NOFT methods, which depend on the occupation numbers,  $\Delta\text{NO}$  recovers static correlation through the occupancy transferred between statically correlated natural orbitals (NOs). Furthermore, the pairing of NOs is based on a small active space, which improves efficiency.

In this work, systems known to be particularly challenging due to static correlation,  $\text{H}_3$  and  $\text{H}_4$  clusters, are used to analyse the performance of  $\Delta\text{NO}$  in conjunction with the dynamic correlation functionals; Colle-Salvetti (CS),<sup>85,88,91</sup> opposite-spin exponential-cusp and Fermi-hole correction (OF),<sup>89,90</sup> Furthermore, it is the aim of this work to provide more

insights into the static correlation challenge through understanding the molecular orbitals and their pairing.

Section 2.2 of this work includes a a brief summary of the  $\Delta$ NO method. The challenging hydrogen clusters and the methods applied are given in Section 2.3. The results for the dissociation and deformation of the studied clusters are presented in Section 2.4. The final Section (2.5) concludes the work presented here.

## 2.2 Theory

### 2.2.1 The $\Delta$ NO Method

The total electronic energy in CFT is constructed based on the cumulant expansion<sup>92</sup> of the two-electron reduced density matrix (2-RDM). Reduced density matrix (RDM) methods consider the use of the one-electron (1-RDM) and two-electron (2-RDM) reduced density matrix as a variable, it can also extend to 3-RDM, 4-RDM, etc. Defining the energy as a functional of 2-RDM is not trivial since the integral elements do not necessarily correspond to an anti-symmetric wave function. However, expressing the energy functional in terms of the 1-RDM makes it easier to maintain an  $N$ -representable function.

The 1-RDM,  $\tilde{\gamma}$ , and 2-RDM,  $\tilde{\Gamma}$ , are expressed in terms of the  $N$ -electron wave function as,

$$\tilde{\gamma}(\mathbf{x}_1, \mathbf{x}'_1) = N \int \Psi^*(\mathbf{x}'_1, \mathbf{x}_2, \mathbf{x}_3, \dots, \mathbf{x}_N) \Psi(\mathbf{x}_1, \mathbf{x}_2, \mathbf{x}_3, \dots, \mathbf{x}_N) d\mathbf{x}_2 \dots d\mathbf{x}_N \quad (2.4a)$$

$$\tilde{\Gamma}(\mathbf{x}_1, \mathbf{x}_2, \mathbf{x}'_1, \mathbf{x}'_2) = \frac{N(N-1)}{2} \int \Psi^*(\mathbf{x}'_1, \mathbf{x}'_2, \mathbf{x}_3, \dots, \mathbf{x}_N) \Psi(\mathbf{x}_1, \mathbf{x}_2, \mathbf{x}_3, \dots, \mathbf{x}_N) d\mathbf{x}_3 \dots d\mathbf{x}_N \quad (2.4b)$$

where  $\Psi$  is a function of the spatial and spin coordinates,  $\mathbf{x} = (\mathbf{r}, \omega)$ . The diagonal of the  $\tilde{\gamma}$  function is the one-electron density, and diagonal of the  $\tilde{\Gamma}$  function is the two-electron density. The 1-RDM is also obtained through the integration of one of the electronic coordinates of the 2-RDM.

The total energy expressed in terms of the 2-RDM is given as,

$$E[\tilde{\Gamma}] = \int [\hat{h}\tilde{\gamma}(\mathbf{x}_1, \mathbf{x}'_1)]_{\mathbf{x}'_1=\mathbf{x}_1} d\mathbf{x}_1 + \int \frac{\tilde{\Gamma}(\mathbf{x}_1, \mathbf{x}_2, \mathbf{x}'_1, \mathbf{x}'_2)}{|\mathbf{r}_1 - \mathbf{r}_2|} d\mathbf{x}_1 d\mathbf{x}_2 \quad (2.5)$$

where the first term is the one-electron energy in which the operator  $\hat{h}$  includes the one-electron kinetic,  $T$ , and potential energy,  $V_{ne}$ , operators of  $M$  nuclei. Defining the energy functional in terms of 1-RDM mitigates the  $N$ -representability issue by restricting the occupation numbers between 0 and 1, as well as their sum to  $N$ . The second term is the two-electron integral that includes the energy of the electronic interactions, which is formally an exact term, but approximated in CFT. This is achieved utilizing the cumulant expansion,

$$\tilde{\Gamma}(\mathbf{x}_1, \mathbf{x}_2, \mathbf{x}'_1, \mathbf{x}'_2) = \tilde{\Gamma}^{(0)}(\mathbf{x}_1, \mathbf{x}_2, \mathbf{x}'_1, \mathbf{x}'_2) + \tilde{\Gamma}_{\text{cum}}(\mathbf{x}_1, \mathbf{x}_2, \mathbf{x}'_1, \mathbf{x}'_2) \quad (2.6)$$

where  $\tilde{\Gamma}^{(0)}(\mathbf{x}_1, \mathbf{x}_2, \mathbf{x}'_1, \mathbf{x}'_2)$  is the zeroth-order term of the 2-RDM expansion,

$$\tilde{\Gamma}^{(0)}(\mathbf{x}_1, \mathbf{x}_2, \mathbf{x}'_1, \mathbf{x}'_2) = \frac{1}{2} [\tilde{\gamma}(\mathbf{x}_1, \mathbf{x}'_1)\tilde{\gamma}(\mathbf{x}_2, \mathbf{x}'_2) - \tilde{\gamma}(\mathbf{x}_1, \mathbf{x}'_2)\tilde{\gamma}(\mathbf{x}_2, \mathbf{x}'_1)]. \quad (2.7)$$

and  $\tilde{\Gamma}_{\text{cum}}(\mathbf{x}_1, \mathbf{x}_2, \mathbf{x}'_1, \mathbf{x}'_2)$  is an unknown recognized as the cumulant. The energy can now be re-expressed as,

$$E^{\Delta\text{NO}} = E_{0-1\text{RDM}}^{\Delta\text{NO}} + E_{\text{cum}}^{\Delta\text{NO}} \quad (2.8)$$

The zeroth-order 1-RDM energy includes contributions of the one-electron energy,  $h_{pp}$ , that contains the kinetic and nuclear potential operator of  $M$  nuclei.  $E_{0-1\text{RDM}}^{\Delta\text{NO}}$  also contains the two-electron energy term. In the basis of the natural orbitals,  $\phi_p$ , and occupancies,  $n_p$ , for open- and closed-shell systems,  $E_{0-1\text{RDM}}^{\Delta\text{NO}}$  is given as,

$$\begin{aligned} E_{0-1\text{RDM}}^{\Delta\text{NO}} = & \sum_p^{cl} 2n_p h_{pp} + \sum_p^{op} n_p h_{pp} + \sum_p^{cl} \sum_q^{cl} n_q n_p (2J_{pq} - K_{pq}) \\ & + \sum_p^{cl} \sum_q^{op} n_p n_q (2J_{pq} - K_{pq}) + \sum_p^{op} \sum_q^{op} \frac{n_p n_q}{2} (J_{pq} - K_{pq}) \end{aligned} \quad (2.9)$$

where

$$h_{pp} = \int \phi_p^*(\mathbf{r}) \left( -\frac{1}{2} \nabla^2 - \sum_A \frac{Z_A}{r_A} \right) \phi_p(\mathbf{r}) d\mathbf{r} \quad (2.10a)$$

$$J_{pq} = \iint \frac{\phi_p^*(\mathbf{r}_1) \phi_q^*(\mathbf{r}_2) \phi_p(\mathbf{r}_1) \phi_q(\mathbf{r}_2)}{r_{12}} d\mathbf{r}_1 d\mathbf{r}_2 \quad (2.10b)$$

$$K_{pq} = \iint \frac{\phi_p^*(\mathbf{r}_1) \phi_q^*(\mathbf{r}_2) \phi_q(\mathbf{r}_1) \phi_p(\mathbf{r}_2)}{r_{12}} d\mathbf{r}_1 d\mathbf{r}_2 \quad (2.10c)$$

In order to construct the cumulant energy term, in the NO basis,  $\Psi_{\Delta\text{NO}}$ , can be expressed as an expansion of Slater determinants.

$$\Psi_{\Delta\text{NO}} = \sum_I c_I \Psi_I \quad (2.11)$$

The electrons can be in their original orbital or in a virtual orbital in a form of 2n-tuply excited determinants,  $\Psi_I$ .

$$\Psi_I = \Psi_{\substack{p\bar{p}q\bar{q}r\bar{r}s\bar{s}\dots \\ i\bar{i}j\bar{j}k\bar{k}l\bar{l}\dots}} \quad (2.12)$$

The product of factors for each double excitation from the active orbitals define the expansion coefficients,  $c_I$ .

$$c_I = d_i^p d_j^q d_k^r \dots \quad (2.13)$$

where the occupied are  $i, j, k, \text{ etc}$  and the virtual are  $p, q, r, \text{ etc}$ .

All elements in Equation (2.11) are defined, thus, the total  $\Delta\text{NO}$  wave function is written as

$$\Psi_{\Delta\text{NO}} = \sum_{pqrs\dots} \left( d_i^p d_j^q d_k^r \dots \right) \Psi_{\substack{p\bar{p}q\bar{q}r\bar{r}s\bar{s}\dots \\ i\bar{i}j\bar{j}k\bar{k}l\bar{l}\dots}} \quad (2.14)$$

where the coefficient factors are defined in terms of occupancies of the NOs or the transfer of electrons from the occupied to virtual NOs,  $\Delta_{ip}$ , as

$$d_i^p = \sqrt{n_i} \delta_{ip} - \sqrt{\Delta_{ip}} \quad (2.15)$$

The occupancy of orbitals,  $n_i$ , that remains after the electronic transfer from an occupied to virtual is expressed as,

$$n_i = 1 - \sum_p \Delta_{ip} \quad (2.16)$$

while the occupancy of a virtual is

$$n_p = \sum_p \Delta_{ip} \quad (2.17)$$

and  $\delta_{ip}$  is the Kronecker delta.

In order to correspond to an  $N$ -electron wave function, the electronic transfer is restricted between 0 and 1.

$$0 \leq \Delta_{ip} \leq 1 \quad (2.18)$$

The total energy,  $E^{\Delta\text{NO}}$ , is found by taking the expectation value of the Hamiltonian with the  $\Delta\text{NO}$  wave function,  $\Psi_{\Delta\text{NO}}$ .

$$\left\langle \Psi_{\Delta\text{NO}} \left| \hat{H} \right| \Psi_{\Delta\text{NO}} \right\rangle = \sum_I d_I^2 H_{II} + \sum_{I \neq J} d_I d_J H_{IJ} \quad (2.19)$$

where the diagonal elements,  $\sum_I d_I^2 H_{II}$ , correspond to both the zeroth-order 1-RDM and the electron pair correction energy terms of  $\Delta\text{NO}$ .

$$\sum_I d_I^2 H_{II} = E_{0\text{-1RDM}}^{\Delta\text{NO}} + E_{\text{pair}}^{\Delta\text{NO}} \quad (2.20)$$

In order to ensure that for fractional occupancies the 2-RDM wave function integrates to the total number of electrons,  $\frac{N(N-1)}{2}$ , the pair correction is introduced. In the NO basis, the  $E_{\text{pair}}^{\Delta\text{NO}}$  energy term is expressed as,

$$E_{\text{pair}}^{\Delta\text{NO}} = \sum_p \sum_q \eta_{pq} (2J_{pq} - K_{pq}) \quad (2.21)$$

where  $\eta_{pq}$  is a pair correction term that is used to remove fictitious correlation interactions and defined as,

$$\begin{aligned} \eta_{pq} = & \delta_{pq} n_p (1 - n_p) + (1 - \delta_{pq}) (\mathbf{O}_p \mathbf{V}_q \Delta_{pq} (n_q - n_p - \Delta_{pq}) \\ & + \mathbf{O}_q \mathbf{V}_p \Delta_{qp} (n_p - n_q - \Delta_{qp}) - \mathbf{V}_p \mathbf{V}_q \sum_r \mathbf{O}_r \Delta_{rp} \Delta_{rq}) \end{aligned} \quad (2.22)$$

where  $\mathbf{O}$  and  $\mathbf{V}$  are vectors that indicate whether an orbital belongs to the occupied or

virtual set.

$$\mathbf{O} = \begin{pmatrix} 1 \\ 1 \\ 1 \\ \vdots \\ 0 \\ 0 \\ 0 \\ \vdots \end{pmatrix}, \mathbf{V} = \mathbf{1} - \mathbf{O} \quad (2.23)$$

where the  $\mathbf{1}$  is a vector with all entries equal to 1.

The second part of the expectation value, Equation (2.19), is the correlation part, which is the cross terms.

$$\sum_{I \neq J} d_I d_J H_{IJ} = \sum_{pqr\dots} \sum_{p'q'r'\dots} \left( d_i^p d_j^q d_k^r \dots \right) \left( d_i^{p'} d_j^{q'} d_k^{r'} \dots \right) \left\langle \Psi_{\bar{i}\bar{j}\bar{k}\bar{l}\dots}^{p\bar{p}q\bar{q}r\bar{r}s\bar{s}\dots} \left| \hat{H} \right| \Psi_{\bar{i}\bar{j}\bar{k}\bar{l}\dots}^{p'p'q'q'r'r's's'\dots} \right\rangle \quad (2.24)$$

The  $\Delta$ NO wave function is derived for disentangled pairing, which means that each active occupied NO is paired with its own exclusive set of vacant orbitals. As a result, the only terms that survive are those that involve the same active occupied orbital,

$$\sum_{I \neq J} d_I d_J H_{IJ} = \sum_{p \neq v} \sum_{qr\dots} d_i^p d_i^v (d_j^q d_k^r \dots)^2 L_{pv} + \sum_{p \neq v} \sum_{pr\dots} d_j^q d_j^v (d_i^p d_k^r \dots)^2 L_{qv} + \dots \quad (2.25)$$

where  $L_{pv}$  is the time-inversion exchange energy integral and expressed as,

$$L_{pv} = \iint \frac{\phi_p^*(\mathbf{r}_1) \phi_p^*(\mathbf{r}_2) \phi_v(\mathbf{r}_1) \phi_v(\mathbf{r}_2)}{r_{12}} d\mathbf{r}_1 d\mathbf{r}_2 \quad (2.26)$$

The sum of squares of the coefficient factors that are with the same active occupied orbital yield one,

$$\sum_p (d_i^p)^2 = \sum_p (\delta_{ip} \sqrt{n_i} - \sqrt{\Delta_{ip}})^2 = n_i + \sum_p \Delta_{ip} = 1 \quad (2.27)$$

Substitution of the definition of the coefficient factors and simplification then leads to,

$$\sum_{I \neq J} d_I d_J H_{IJ} = \sum_{p \neq v} (\sqrt{n_i} \delta_{ip} - \sqrt{\Delta_{ip}}) (\sqrt{n_i} \delta_{iv} - \sqrt{\Delta_{iv}}) L_{pv} \quad (2.28a)$$

$$E_{\text{stat}}^{\Delta\text{NO}} = - \sum_{ip} \sqrt{n_i \Delta_{ip}} (L_{ip} + L_{pi}) + \sum_{p \neq q} \sum_i \sqrt{\Delta_{ip} \Delta_{iq}} L_{pq} \quad (2.28b)$$

The energy of the  $\Delta\text{NO}$  wave function then becomes,

$$\begin{aligned} \left\langle \Psi_{\Delta\text{NO}} \left| \hat{H} \right| \Psi_{\Delta\text{NO}} \right\rangle &= E_{0\text{-1RDM}}^{\Delta\text{NO}} + E_{\text{pair}}^{\Delta\text{NO}} + E_{\text{stat}}^{\Delta\text{NO}} \\ &= \sum_p^{cl} 2n_p h_{pp} + \sum_p^{op} n_p h_{pp} + \sum_p^{cl} \sum_q^{cl} n_p n_q (2J_{pq} - K_{pq}) \\ &\quad + \sum_p^{cl} \sum_q^{op} n_p n_q (2J_{pq} - K_{pq}) + \sum_p^{op} \sum_q^{op} \frac{n_p n_q}{2} (J_{pq} - K_{pq}) \\ &\quad + \sum_p \sum_q \eta_{pq} (2J_{pq} - K_{pq}) + \sum_{pq} (\zeta_{pq} - \xi_{pq}) L_{pq} \end{aligned} \quad (2.29)$$

where the coefficients of the static correlation term are defined as,

$$\zeta_{pq} = V_p V_q \sum_r \sqrt{\Delta_{rp} \Delta_{rq}} \quad (2.30a)$$

$$\xi_{pq} = O_p V_q \sqrt{n_p \Delta_{pq}} + V_p O_q \sqrt{n_q \Delta_{qp}} \quad (2.30b)$$

In order to ensure that bonds are dissociated properly in the framework of  $\Delta\text{NO}$ , it is necessary to include a correction (Equation 2.30) to the description of bond dissociation. Therefore, high-spin correction (HSC) energy is introduced. HSC is necessary to increase the pair density between parallel-spin electrons while decreasing the pair density of antiparallel-spin electrons of statically correlated electron pairs. It ensures that in molecular dissociation, the statically correlated electrons remain in a high-spin state locally on the separated atoms. If the correction is missing, an average of both high- and low-spin states would be included, which would lead to inaccurate computed energies.

$$E_{\text{HSC}}^{\Delta\text{NO}} = - \sum_{pq} \kappa_{pq} K_{pq} \quad (2.31)$$

where

$$\kappa_{pq} = (O_p O_q + V_p V_q) \sum_{r \neq s} \xi_{pr} \xi_{qs} + O_p V_q \sum_{\substack{r(\neq q) \\ s(\neq p)}} \xi_{pr} \xi_{sq} + V_p O_q \sum_{\substack{r(\neq q) \\ s(\neq p)}} \xi_{rp} \xi_{qs} \quad (2.32)$$

The final energy term,  $E_{\text{dyn}}^{\Delta\text{NO}}$ , in the proposed cumulant energy is based on the on-top two-electron dynamic correlation functionals; CS<sup>85,88,91</sup> and OF.<sup>89,90</sup> These functionals account for short-range dynamic correlation energy,  $E_{\text{sr-dyn}}$ ; and thus, the long-range dynamic correlation energy is still not implemented in  $\Delta\text{NO}$  and remains for future work.

$$E_{\text{dyn}}^{\Delta\text{NO}} = E_{\text{CS/OF}}^{\Delta\text{NO}} \quad (2.33)$$

Combining the derived energy terms leads to the final proposed  $\Delta\text{NO}$  cumulant energy expression.

$$E_{\text{cum}}^{\Delta\text{NO}} = E_{\text{pair}}^{\Delta\text{NO}} + E_{\text{stat}}^{\Delta\text{NO}} + E_{\text{HSC}}^{\Delta\text{NO}} + E_{\text{dyn}}^{\Delta\text{NO}} \quad (2.34)$$

## 2.3 Methods

Potential energy surfaces (PESs) of the dissociation of linear  $\text{H}_3$  ( $C_{\infty v}$ ) and  $\text{H}_4$  ( $D_{\infty h}$ ) and square  $\text{H}_4$  ( $D_{4h}$ ) are analyzed as a function of internuclear distance ( $R$ ) between the H atoms, while the PES of  $\text{H}_4$  with rectangle to square geometry ( $D_{2h}/D_{4h}$ ) is given as a function of  $\theta$ , which controls the angles between two adjacent H atoms, see Figure 2.1. Such systems have been previously used to evaluate the performance of DFT, post-HF, and other methods.<sup>25,93–95</sup> Stretching systems of  $\text{H}_3$  and  $\text{H}_4$  becomes more challenging at larger bond lengths where the multireference character becomes more substantial.<sup>71,96</sup> As for  $\text{H}_4$ , transitioning from rectangle to square is more statically correlated, where if modelled incorrectly, there is a cusp in energy at  $\theta = 90$ .<sup>72–74</sup>

The absolute energies of full CI, B3LYP, and CCSD(T) methods were computed using GAMESS,<sup>97</sup> while the  $\Delta\text{NO}$  calculations were performed using MUNgauss.<sup>98</sup> The  $\Delta\text{NO}$  calculations include the aforementioned dynamic correlation functionals; CS and OF, corresponding to  $\Delta\text{NO-CS}$  and  $\Delta\text{NO-OF}$ , respectively. To properly recover correlation, the

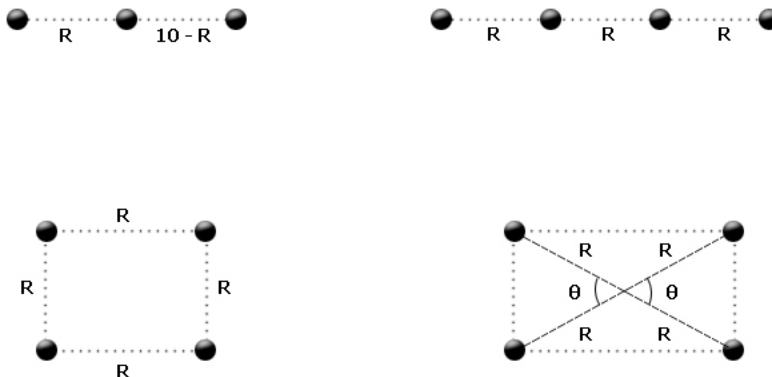


Figure 2.1: Challenging systems of H clusters. From top left,  $H_3$   $C_{\infty v}$ ,  $H_4$ ;  $D_{\infty h}$ ,  $D_{4h}$  and  $D_{2h}/D_{4h}$ .  $R$  in Å.

Dunning’s correlation consistent, polarized valence, triple zeta basis sets (cc-pVTZ) is selected for all calculations.<sup>99–101</sup>

## 2.4 Results and Discussion

For each linear H cluster ( $C_{\infty v}$  and  $D_{\infty h}$ ) and  $H_4$  square ( $D_{4h}$ ) cluster, the performance of the methods relative to full CI on the PES, equilibrium bond length ( $R_e$ ) and its corresponding energy ( $E$ ), dissociation energy ( $D_e$ ), and difference in absolute energies ( $E_{\text{Full CI}} - E_{\Delta\text{NO}}$ ) is discussed. In addition to that, for the  $H_4$   $D_{2h}/D_{4h}$  cluster, relative energy values ( $E_{\text{Full CI}}[\theta] - E_{\Delta\text{NO}}[\theta]$ ), and energy barrier is reported. The dissociation energy curves for the  $H_3$  molecule by  $\Delta\text{NO}$ , with both CS and OF dynamic energy functionals, full CI, and B3LYP are given in Figure 2.2. Table 2.1 includes  $R_e$  and energies calculated using the aforementioned methods. Moreover,  $D_e$  are reported in Table 2.2.

The calculated  $R_e$  at  $\Delta\text{NO}$  is in agreement with full CI, where the difference does not exceed 0.003 Å. On the other hand, the  $\Delta\text{NO}$ –CS overestimates the dynamic correlation energy where at  $R_e$ ,  $E_{\text{Full CI}} - E_{\Delta\text{NO-CS}} = 0.00441$  (12 kJ mol<sup>-1</sup>). This is also reflected on  $D_e = 465$  kJ mol<sup>-1</sup>, which is overestimated by 11 kJ mol<sup>-1</sup> due to double counting. The  $\Delta\text{NO}$ –OF, however, is in excellent agreement with full CI where the difference in energy at

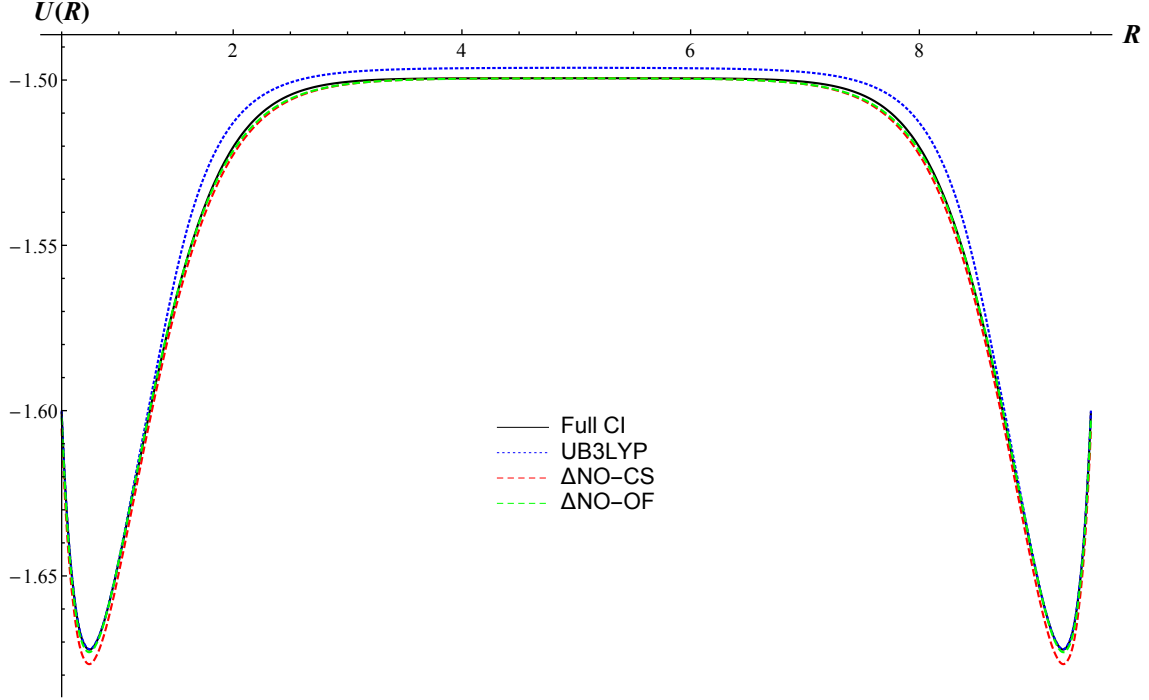


Figure 2.2: Potential energy surface of  $\text{H}_3$  as a function of  $R$  ( $\text{\AA}$ ).

$R_e$  is  $2 \text{ kJ mol}^{-1}$ , and  $D_e = 455 \text{ kJ mol}^{-1}$  is comparable to full CI predicted value of  $454 \text{ kJ mol}^{-1}$ .

The dynamic correlation decays as the system is stretched, where at the dissociation limit,  $\Delta\text{NO-CS}$ , similar to  $\Delta\text{NO-OF}$ , coincides with the full CI curve, which means that  $\Delta\text{NO}$  properly describes the dissociation of the molecule and accounts well for  $E_{\text{stat}}$ . UB3LYP

Table 2.1: Equilibrium bond lengths ( $\text{\AA}$ ) and minimum energies (hartree) of different hydrogen systems.

Molecule	Full CI		UB3LYP		$\Delta\text{NO-CS}$		$\Delta\text{NO-OF}$	
	$R_e$	$E$	$R_e$	$E$	$R_e$	$E$	$R_e$	$E$
$\text{H}_3(C_{\infty v})$	0.743	-1.67227	0.744	-1.67213	0.741	-1.67668	0.740	-1.67307
$\text{H}_4(D_{\infty h})$	0.884	-2.27822	0.883	-2.28648	0.878	-2.2801	0.880	-2.27504
$\text{H}_4(D_{4h})$	0.863	-2.10891	0.842	-2.12798	0.853	-2.1126	0.860	-2.10929

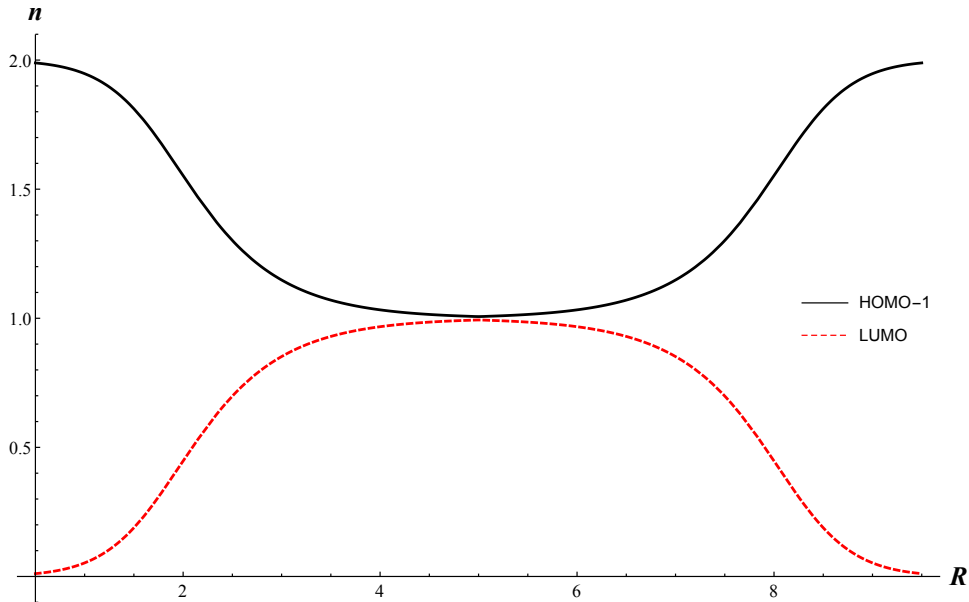


Figure 2.3: Change in occupation numbers of statically correlated NOs of  $\text{H}_3$  as a function of  $R$  ( $\text{\AA}$ ).

correctly predicts both of  $R_e$  and energy, however, the dissociation energy,  $D_e = 461 \text{ kJ mol}^{-1}$ , is slightly higher. It also dissociates the molecule rapidly, compared to full CI.

In the ROHF wave function, the first MO of  $\text{H}_3$  (HOMO-1) is doubly occupied, and the second (HOMO) is singly occupied. The  $\Delta\text{NO}$  method pairs the HOMO-1 with LUMO. The transfer of electrons is initiated from HOMO-1, to the LUMO, see Figure 2.3. At around  $1.000 \text{ \AA}$ , the change of occupancies occurs, and as the system is stretched,  $E_{\text{stat}}$  increases dramatically, whereas  $E_{\text{dyn}}$  decreases significantly. At complete bond dissociation,  $5.000 \text{ \AA}$ , both orbitals are half filled, each with one electron (Figure 2.3). Moreover, the HOMO is

Table 2.2: Dissociation energies ( $\text{kJ mol}^{-1}$ ) of different hydrogen systems.

Molecule	Full CI	UB3LYP	$\Delta\text{NO-CS}$	$\Delta\text{NO-OF}$
$\text{H}_3(C_{\infty v})$	454	461	465	455
$\text{H}_4(D_{\infty h})$	732	764	734	721
$\text{H}_4(D_{4h})$	288	349	298	289

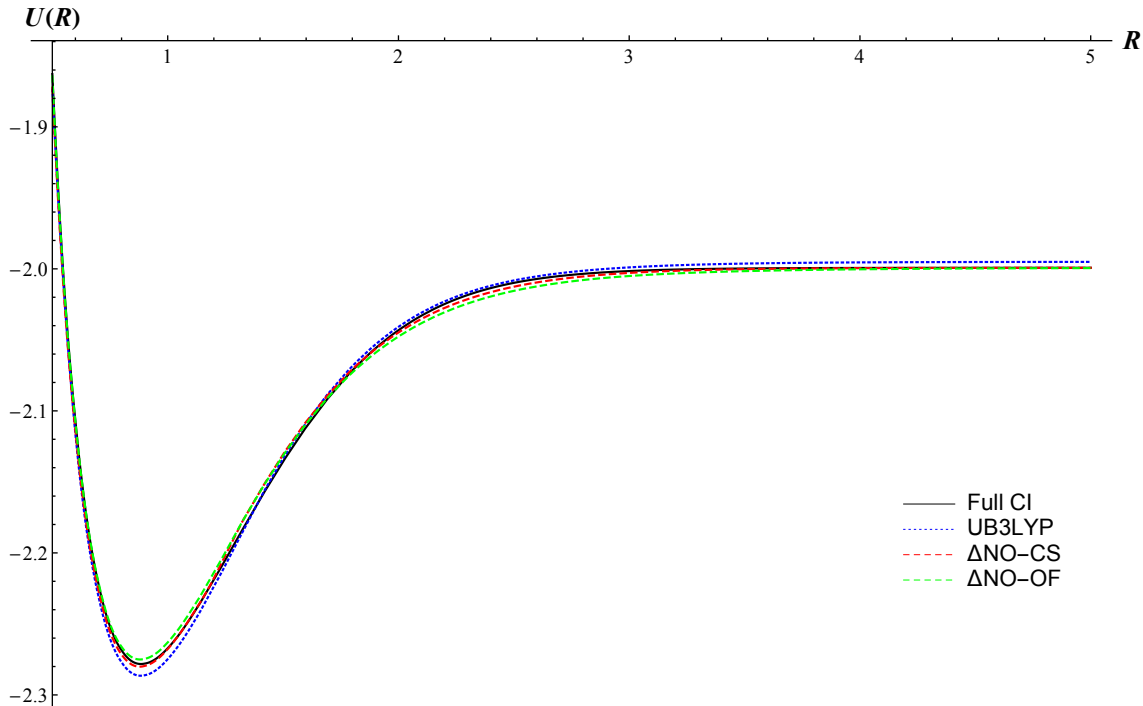


Figure 2.4: Potential energy surface of  $H_4$  as a function of  $R$  ( $\text{\AA}$ ).

already filled with one electron, which means that degeneracy of the statically correlated NOs occurs between HOMO, HOMO-1, and LUMO.

The dissociation energy curve for linear  $H_4$  molecule as a function of  $R$  is given in Figure 2.4. The system begins with a HF configuration of  $a_g^2 b_{3u}^2$ , while stretching the molecule, both HF configurations of  $a_g^2 b_{3u}^2$  and  $a_g^2 b_{2u}^2$  become degenerate and equally important. Conventional electronic structure methods fail to describe such system because of the single Slater determinant nature.

The PES shows that the  $\Delta\text{NO-CS}$  dissociates the molecule similar to full CI, whereas  $\Delta\text{NO-OF}$  slightly falls under the full CI curve,  $1.7 \leq R \leq 2.4$ , but recovers at complete dissociation where  $E_{\text{stat}}$  is dominant.  $\Delta\text{NO-CS}$  predicts a somewhat lower value of  $R_e = 0.878 \text{ \AA}$  to the value of full CI, this is also observed at  $\Delta\text{NO-OF}$  where the  $R_e$  is off by  $0.004 \text{ \AA}$ . Although UB3LYP overestimates  $E_{\text{dyn}}$  at equilibrium, the predicted  $R_e = 0.883 \text{ \AA}$  is in agreement with full CI. In terms of energies,  $\Delta\text{NO}$  is close to full CI where at  $R_e$ ,  $E_{\text{Full CI}} - E_{\Delta\text{NO-CS}} = 0.00187$  ( $5 \text{ kJ mol}^{-1}$ ) and  $E_{\text{Full CI}} - E_{\Delta\text{NO-OF}} = 0.00318$  ( $8 \text{ kJ mol}^{-1}$ ).

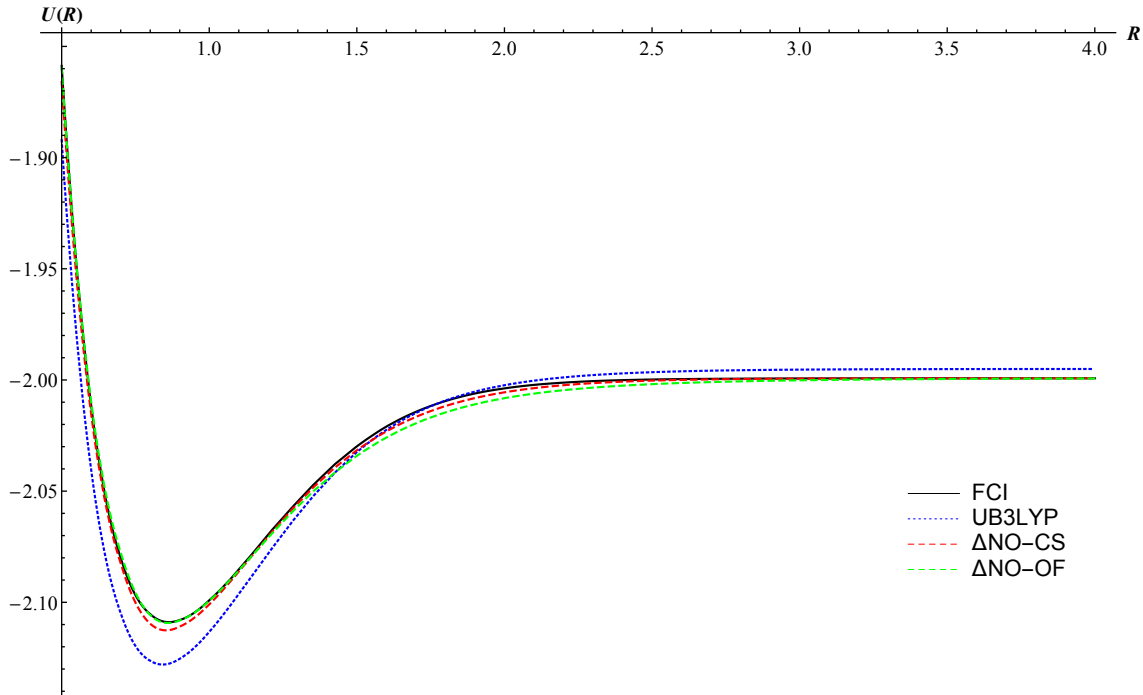


Figure 2.5: Potential energy surface of square  $H_4$  ( $D_{4h}$ ) as a function of  $R$  ( $\text{\AA}$ ).

In contrast, the predicted UB3LYP results are significantly lower than full CI energies by  $22 \text{ kJ mol}^{-1}$ . This is also observed for the value of  $D_e$  where the energy is higher by  $32 \text{ kJ mol}^{-1}$ . As for  $\Delta\text{NO-CS}$ , the calculated  $D_e$  is close to full CI, however,  $\Delta\text{NO-OF}$  predicts a lower value by  $11 \text{ kJ mol}^{-1}$ .

The change in occupation numbers in  $H_4$  from  $b_{3u}$  to  $b_{2u}$  is qualitatively similar to  $H_3$  (Figure A.1), where all linear systems stretched in a similar regime exhibit this.

The dissociation energy curve for the square  $H_4$  ( $D_{4h}$ ) molecule as a function of  $R$  is given in Figure 2.5. The predicted  $\Delta\text{NO-CS}$  value of  $R_e = 0.853 \text{ \AA}$  is lower by  $0.010 \text{ \AA}$  than the calculated at full CI (Table 2.1). The energy is also overestimated at that region, where it could be attributed to the double counting of  $E_c$ , which also affects  $D_e$  that is overestimated by  $10 \text{ kJ mol}^{-1}$  (Table 2.2). However,  $\Delta\text{NO-OF}$  predicts  $R_e = 0.860 \text{ \AA}$ , which is comparable to the full CI value of  $0.863 \text{ \AA}$ . This agreement is also observed for the absolute energies as well as  $D_e$ , where the difference is negligible;  $1 \text{ kJ mol}^{-1}$ . UB3LYP fails to describe this system drastically. Although  $R_e$  is far from full CI by  $0.020 \text{ \AA}$ , the electronic energy is

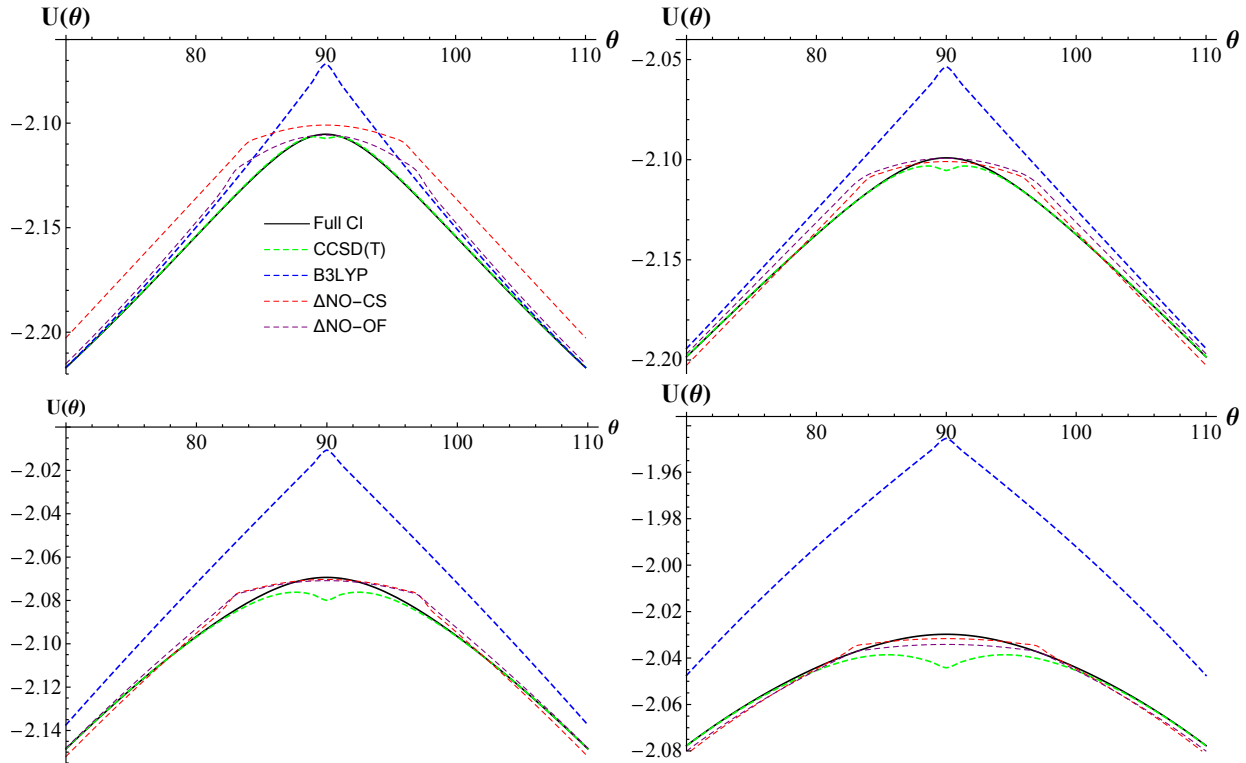


Figure 2.6: Potential energy surface of  $H_4$  ( $D_{2h}/D_{4h}$ ), top left  $R = 0.8, 1.0 \text{ \AA}$  bottom left  $R = 1.2, 1.5 \text{ \AA}$ , as a function of  $\theta$ .

significantly higher by  $50 \text{ kJ mol}^{-1}$ . Moreover, the calculated  $D_e$  value is higher by  $61 \text{ kJ mol}^{-1}$ .

The HF configuration of the square  $H_4$  ( $D_{4h}$ ) is  $a_g^2 b_{2u}^1 b_{3u}^1$ . In using  $\Delta NO$ , the selected pairing for the electronic transfer is from  $a_g$  to  $b_{1g}$ , which occurs by stretching the system up until all electrons are populated with one electron with a configuration of  $a_g^1 b_{2u}^1 b_{3u}^1 b_{1g}^1$ . The transfer of electrons is qualitatively similar to  $H_3$ , however, the change in occupation numbers begin at  $0.600 \text{ \AA}$ , see Figure A.2.

In Figure 2.6 the  $\Delta NO$  PES of  $H_4$  ( $D_{2h}/D_{4h}$ ) as a function of  $\theta$  while  $R$  remains fixed is compared to full CI, B3LYP, and CCSD(T). As the system's radius increases, the potential energies become flat and  $E_{\text{stat}}$  is severe. The performance of different functionals is included in this figure to show their general description of the energies. At  $\theta = 70^\circ$ , the system has a  $D_{2h}$  point group with a HF configuration of  $a_g^2 b_{3u}^2$ . As  $\theta$  is varied up to  $90^\circ$ , the point

Table 2.3:  $\Delta E$  values ( $\text{kJ mol}^{-1}$ ) as a function of  $\theta$  for  $\text{H}_4$  ( $D_{2h}/D_{4h}$ ).

$R = 0.8 \text{ \AA}$					$R = 1.0 \text{ \AA}$			
$\theta^\circ$	B3LYP <sup>†</sup>	CCSD(T) <sup>†</sup>	$\Delta\text{NO-CS}^\dagger$	$\Delta\text{NO-OF}^\dagger$	B3LYP <sup>†</sup>	CCSD(T) <sup>†</sup>	$\Delta\text{NO-CS}^\dagger$	$\Delta\text{NO-OF}^\dagger$
70	-0.25	-0.42	-37.41	-4.98	-10.94	-0.39	11.09	-4.02
90	-88.52	5.25	-11.53	0.98	-119.56	16.54	4.82	0.56
$R = 1.2 \text{ \AA}$					$R = 1.5 \text{ \AA}$			
70	-29.08	-0.25	9.29	-0.98	-79.35	0.21	9.80	6.15
90	-154.31	27.80	2.50	3.92	-221.45	37.86	4.89	11.46
$R = 1.7 \text{ \AA}$					$R = 2.2 \text{ \AA}$			
70	-128.85	0.53	10.34	9.72	-273.24	0.63	-3.86	2.28
90	-274.35	35.94	6.08	13.65	-395.85	17.06	3.02	8.92
$R = 3.0 \text{ \AA}$								
70	-433.13	—	0.36	3.16				
90	-494.60	—	0.22	2.17				

<sup>†</sup>  $\Delta E[\theta] = \text{Full CI}[\theta] - \text{X}[\theta]$ . — Does not converge.

group becomes  $D_{4h}$ , where the system is completely symmetric and is described by degenerate orbitals with a HF configuration of  $a_g^2 b_{2u}^1 b_{3u}^1$ . As it becomes dominated by degeneracy, conventional methods; HF, DFT, CC, and MP2 fail to describe the smooth energies, such as the calculated values by full CI, and represent the PES with a cusp in energy at  $\theta = 90^\circ$ . The transition from  $D_{2h}$  to  $D_{4h}$  is challenging since it becomes significantly statically correlated.

The predicted results of  $\Delta\text{NO}$  are not only quantitatively right but also qualitatively, where the energies are smooth in the vicinity of  $\theta = 90^\circ$ . Furthermore,  $\Delta\text{NO-OF}$  calculated energies excel the predicted energies of  $\Delta\text{NO-CS}$  with closer values to full CI, where the latter underestimates  $U(\theta = 70^\circ)$  by no more than  $37 \text{ kJ mol}^{-1}$ , at different  $R$  values (Table 2.3). However, at  $R \geq 1.0 \text{ \AA}$  it exhibits an obvious change in energies, which is due to the fact that the paired orbitals change symmetry for  $U(\theta < 86^\circ)$  and another for  $U(86^\circ \geq \theta \leq 90^\circ)$ . The developed  $\Delta\text{NO}$  theory captures these energies without a modification of orbital sets, where  $a_g$  is paired with  $b_{2u}$  and  $b_{3u}$  is with  $b_{1g}$ . However, at certain points, the paired orbitals symmetry changes upon optimization. This is initially observed at  $R = 1.0 \text{ \AA}$ , until

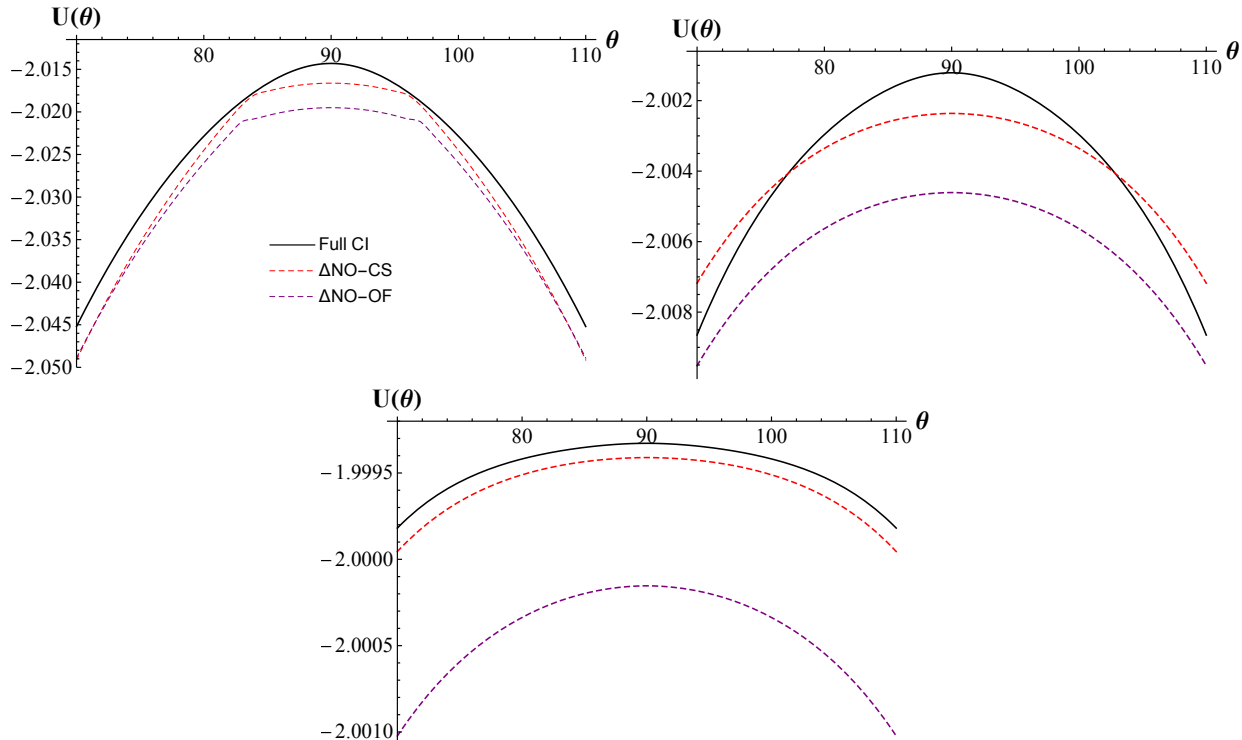


Figure 2.7: Potential energy surface of  $H_4$  ( $D_{2h}/D_{4h}$ ), top left counter clockwise  $R = 1.7, 2.2, 3.0 \text{ \AA}$ , as a function of  $\theta$ .

$R$  becomes equal to  $2.0 \text{ \AA}$ , see Figures 2.6 and 2.7.

The qualitative performance of B3LYP is incorrect with a convex cusp in energy at  $\theta = 90^\circ$ , whereas CCSD(T) energies result in a concave cusp. Both methods lead to incorrect results; however, for  $\theta \leq 80^\circ$  the energies computed at CCSD(T) are close to full CI. On the other hand, when  $R \geq 3.0 \text{ \AA}$  it becomes difficult to converge CCSD(T) energies. Table 2.3 shows how the change in  $R$  affects the energies. Moreover, as  $R$  is increased and  $\theta$  is varied on the PES,  $U(\theta)$ , static correlation dominates even more and this improper description of the PES by B3LYP and CCSD(T) increases significantly, not only qualitatively but also quantitatively.

The difference in energy between B3LYP/CCSD(T) and full CI,  $\Delta E[\theta = 70^\circ]$ , is negligible. However, at  $R = 3.0 \text{ \AA}$ ,  $\Delta E[\theta = 70^\circ \text{ and } 90^\circ]$  of B3LYP energies becomes  $-433 \text{ kJ mol}^{-1}$ . Computed CCSD(T) energies remain consistent with full CI at  $\theta = 70^\circ$ ; however, as

Table 2.4: The difference in absolute energies at  $\theta = 90^\circ$  and  $70^\circ$  ( $\text{kJ mol}^{-1}$ ) for  $\text{H}_4$  ( $D_{2h}/D_{4h}$ ). Basis set aug-cc-pVDZ.

$R$ ( $\text{\AA}$ )	Full CI*	PNOF6*	$\Delta\text{NO-CS}$	$\Delta\text{NO-OF}$
0.8	288	310	346	331
1.0	257	289	267	256
1.2	205	242	215	203

\* Reference<sup>74</sup>

the minimum cusp increases on the PES,  $\Delta E[\theta = 90^\circ]$  becomes larger reaching a value of  $32 \text{ kJ mol}^{-1}$ , until the PES becomes flat at  $R = 2.2 \text{ \AA}$  where  $\Delta E[\theta = 90^\circ] = 17.06 \text{ kJ mol}^{-1}$ .

$\Delta\text{NO-OF}$  shows considerable consistency compared to full CI at  $\theta = 70^\circ$ , where  $\Delta E[\theta]$  does not exceed  $10 \text{ kJ mol}^{-1}$ , as  $R \rightarrow 3.0 \text{ \AA}$ . At  $\theta = 90^\circ$ , the performance is still adequate (Figure 2.7), however, the only considerable difference in  $\Delta E[\theta]$  is at  $1.5$  and  $1.7 \text{ \AA}$ , where the calculated relative energy values are  $11$  and  $13 \text{ kJ mol}^{-1}$ , respectively. This could be attributed to the shift in energies at  $\theta = 84^\circ$  and  $96^\circ$ . This is also observed in a natural orbital functional method, PNOF6;<sup>74</sup> however, in their case it is explained as having two solutions of energies that are being combined. A comparison of energies relative to full CI is made between PNOF6 and  $\Delta\text{NO}$  in Table 2.4. The only case where PNOF6 deals with the relative energies better is at  $R = 0.8 \text{ \AA}$ . However, at all other  $R$  values,  $\Delta\text{NO}$  outperforms PNOF6, where the relative energy barrier is in agreement with full CI.

## 2.5 Conclusions

The  $\Delta\text{NO}$  method successfully deals with systems that require a multireference approach effectively, while maintaining disjoint orbital pairing through the PESs investigated. It is also superior to B3LYP and CCSD(T), particularly, in square  $\text{H}_4$  ( $D_{4h}$ ) and rectangle to square ( $D_{2h}/D_{4h}$ ).

The calculations made by  $\Delta\text{NO}$  of equilibrium bond lengths, absolute and dissociation

energies are  $H_3$  and  $H_4$  systems are accurate and in agreement with full CI. The occupation numbers change smoothly with correct description of the PES given as function of bond length. However, occupation numbers of  $H_4$  ( $D_{2h}/D_{4h}$ ) are not entirely smooth. This is due to the change in the paired orbitals symmetry that occurs from  $\theta = 86^\circ$  to  $\theta = 94^\circ$ .

For linear systems, UB3LYP performs well for  $H_3$ , however, its performance is less impressive with  $H_4$ . For  $H_3$ , estimations made by  $\Delta\text{NO-OF}$  are comparable to UB3LYP. For  $H_4$ , on the other hand,  $\Delta\text{NO}$  exceeds the performance of UB3LYP, in terms of energies and equilibrium bond lengths. This is due to the dynamic correlation functional, LYP, incorporated in B3LYP, where it overcorrelates the energies as the number of electrons increases.

The significant challenge begins for B3LYP at the square  $H_4$  ( $D_{4h}$ ) cluster. Although the qualitative description of the energies is incorrect to begin with because of the cusp in energy that has been illustrated at  $\theta = 90^\circ$ , the energies are severely overcorrelated at the equilibrium region and underestimated at the dissociation limit. Moreover, the computed equilibrium bond length is higher than the predicted bond length of full CI. The CCSD(T) method is not capable of describing this system as it does not converge. This is due to the degeneracy of the orbitals, and the static correlation that increases as the bond length is stretched. The predicted energies of  $\Delta\text{NO}$  outperform these methods and compare to full CI with correct dissociation of the molecule.

The PES of  $H_4$  ( $D_{2h}/D_{4h}$ ) has been modelled smoothly by  $\Delta\text{NO}$  that also shows a correct molecular dissociation, unlike conventional methods which shows a cusp in energy at the transition of  $D_{2h} \rightarrow D_{4h} \rightarrow D_{2h}$ . Furthermore,  $\Delta\text{NO}$  estimated energies are in agreement with full CI, which shows that the dynamic correlation functionals reliable in accounting for  $E_{\text{dyn}}$ .

# References

- [1] Raghavachari, K. Electron Correlation Techniques in Quantum Chemistry: Recent Advances. *Annu. Rev. Phys. Chem.* **1991**, *42*, 615–642.
- [2] Raghavachari, K.; Anderson, J. B. Electron Correlation Effects in Molecules. *J. Phys. Chem.* **1996**, *100*, 12960–12973.
- [3] Tew, D. P.; Klopper, W.; Helgaker, T. Electron Correlation: The Many-Body Problem at the Heart of Chemistry. *J. Comput. Chem.* **2007**, *28*, 1307–1320.
- [4] Kohn, W.; Becke, A. D.; Parr, R. G. Density Functional Theory of Electronic Structure. *J. Phys. Chem.* **1996**, *100*, 12974–12980.
- [5] Geerlings, P.; Proft, F. D.; Langenaeker, W. Conceptual Density Functional Theory. *Chem. Rev.* **2003**, *103*, 1793–1874.
- [6] Becke, A. D. Perspective: Fifty years of density-functional theory in chemical physics. *J. Chem. Phys.* **2014**, *140*, 18A301.
- [7] Cohen, J. A.; Mori-Sánchez, P.; Yang, W. Challenges for Density Functional Theory. *Chem. Rev.* **2012**, *112*, 289–320.
- [8] Hachmann, J.; Cardoen, W.; Chan, G. K.-L. Multireference correlation in long molecules with the quadratic scaling density matrix renormalization group. *J. Chem. Phys.* **2006**, *125*, 144101.

- [9] Tsuchimochi, T.; Scuseria, G. E. Strong correlations via constrained-pairing mean-field theory. *J. Chem. Phys.* **2009**, *131*, 121102.
- [10] Sinitskiy, A. V.; Greenman, L.; Mazziotti, D. A. Strong correlation in hydrogen chains and lattices using the variational two-electron reduced density matrix method. *J. Chem. Phys.* **2010**, *133*, 014104.
- [11] Stella, L.; Attaccalite, C.; Sorella, S.; Rubio, A. Strong electronic correlation in the hydrogen chain: A variational Monte Carlo study. *Phys. Rev. B* **2011**, *84*, 245117.
- [12] Motta, M. et al. Towards the Solution of the Many-Electron Problem in Real Materials: Equation of State of the Hydrogen Chain with State-of-the-Art Many-Body Methods. *Phys. Rev. X* **2017**, *7*, 031059.
- [13] Mitxelena, I.; Piris, M. An efficient method for strongly correlated electrons in two-dimensions. *J. Chem. Phys.* **2020**, *152*, 064108.
- [14] Boguslawski, K.; Tecmer, P.; Ayers, P. W.; Bultinck, P.; De Baerdemacker, S.; Van Neck, D. Efficient description of strongly correlated electrons with mean-field cost. *Phys. Rev. B* **2014**, *89*, 201106.
- [15] Mitxelena, I.; Piris, M. An efficient method for strongly correlated electrons in two-dimensions. *J. Chem. Phys.* **2020**, *152*, 064108.
- [16] Kong, J.; Proynov, E.; Yu, J.; Pachter, R. Describing a Strongly Correlated Model System with Density Functional Theory. *J. Phys. Chem. Lett.* **2017**, *8*, 3142–3146.
- [17] Löwdin, P.-O. Discussion on the Hartree-Fock approximation. *Rev. Mod. Phys.* **1963**, *35*, 496–501.
- [18] Crittenden, D. L. A Hierarchy of Static Correlation Models. *J. Phys. Chem. A* **2013**, *117*, 3852–3860.

- [19] Benavides-Riveros, C. L.; Lathiotakis, N. N.; Marques, M. A. L. Towards a Formal Definition of Static and Dynamic Electronic Correlations. *Phys. Chem. Chem. Phys.* **2017**, *19*, 12655.
- [20] Ramos-Cordoba, E.; Salvador, P.; Matito, E. Separation of Dynamic and Nondynamic Correlation. *Phys. Chem. Chem. Phys.* **2016**, *18*, 24015.
- [21] Via-Nadal, M.; Rodriguez-Mayorga, M.; Ramos-Cordoba, E.; Matito, E. Singling Out Dynamic and Nondynamic Correlation. *J. Phys. Chem. Lett.* **2019**, *10*, 4032.
- [22] Mok, D. K. W.; Neumann, R.; Handy, N. C. Dynamical and Nondynamical Correlation. *J. Phys. Chem.* **1996**, *100*, 6225–6230.
- [23] Handy, N. C.; Cohen, A. J. Left-right correlation energy. *Mol. Phys.* **2001**, *99*, 403–412.
- [24] Tsuchimochi, T.; Voorhis, T. V. Extended Møller-Plesset perturbation theory for dynamical and static correlations. *J. Chem. Phys.* **2014**, *141*, 164117.
- [25] Kong, J.; Proynov, E. Density Functional Model for Nondynamic and Strong Correlation. *J. Chem. Theory Comput.* **2016**, *12*, 133–143.
- [26] Sinanoğlu, O. *Advances in Chemical Physics*; 2007; Chapter 7, pp 315–412.
- [27] Molawi, K.; Cohen, A. J.; Handy, N. C. Left-right and dynamic correlation. *Int. J. Quantum Chem.* **2002**, *89*, 86–93.
- [28] Becke, A. D. Density functionals for static, dynamical, and strong correlation. *J. Chem. Phys.* **2013**, *138*, 074109.
- [29] Phillips, J. J.; Zgid, D. The description of strong correlation within self-consistent Green's function second-order perturbation theory. *J. Chem. Phys.* **2014**, *140*, 241101–241107.
- [30] Wallace, A. J.; Crittenden, D. L. Optimal Composition of Atomic Orbital Basis Sets for Recovering Static Correlation Energies. *J. Phys. Chem. A* **2014**, *118*, 2138–2148.

- [31] Hollett, J. W.; Gill, P. M. W. The two faces of static correlation. *J. Chem. Phys.* **2011**, *134*, 114111.
- [32] Zhao, L.; Neuscamman, E. Amplitude Determinant Coupled Cluster with Pairwise Doubles. *J. Chem. Theory Comput.* **2016**, *12*, 5841–5850.
- [33] Piris, M.; Lopez, X.; Ugalde, J. M. The Bond Order of C2 from a Strictly N-Representable Natural Orbital Energy Functional Perspective. *Chem. Eur. J* **2016**, *22*, 4109–4115.
- [34] Koch, D.; Fertitta, E.; Paulus, B. Calculation of the static and dynamical correlation energy of pseudo-one-dimensional beryllium systems via a many-body expansion. *J. Chem. Phys.* **2016**, *145*, 024104.
- [35] Bytautas, L.; Scuseria, G. E.; Ruedenberg, K. Seniority number description of potential energy surfaces: Symmetric dissociation of water, N2, C2, and Be2. *J. Chem. Phys.* **2015**, *143*, 094105.
- [36] Lopez, X.; Ruipérez, F.; Piris, M.; Matxain, J. M.; Matito, E.; Ugalde, J. M. Performance of PNOF5 Natural Orbital Functional for Radical Formation Reactions: Hydrogen Atom Abstraction and C–C and O–O Homolytic Bond Cleavage in Selected Molecules. *J. Chem. Theory Comput.* **2012**, *8*, 2646–2652.
- [37] Zen, A.; Coccia, E.; Luo, Y.; Sorella, S.; Guidoni, L. Static and Dynamical Correlation in Diradical Molecules by Quantum Monte Carlo Using the Jastrow Antisymmetrized Geminal Power Ansatz. *J. Chem. Theory Comput.* **2014**, *10*, 1048–1061.
- [38] Mullinax, J. W.; Sokolov, A. Y.; III, H. F. S. Can Density Cumulant Functional Theory Describe Static Correlation Effects? *J. Chem. Theory Comput.* **2015**, *11*, 2487–2495.
- [39] Smart, S. E.; Scrape, P. G.; Butler, L. J.; Mazziotti, D. A. Using reduced density matrix techniques to capture static and dynamic correlation in the energy landscape

- for the decomposition of the CH<sub>2</sub>CH<sub>2</sub>ONO radical and support a non-IRC pathway. *J. Chem. Phys.* **2018**, *149*, 024302.
- [40] Carlson, R. K.; Truhlar, D. G.; Gagliardi, L. Multiconfiguration Pair-Density Functional Theory: A Fully Translated Gradient Approximation and Its Performance for Transition Metal Dimers and the Spectroscopy of Re<sub>2</sub>Cl<sub>8</sub><sup>2-</sup>. *J. Chem. Theory Comput.* **2015**, *11*, 4077–4085.
- [41] Schlingen, A. W.; Mazziotti, D. A. Static and Dynamic Electron Correlation in the Ligand Noninnocent Oxidation of Nickel Dithiolates. *J. Phys. Chem. A* **2017**, *121*, 9377–9384.
- [42] Chu, S.; Bovi, D.; Cappelluti, F.; Orellana, A. G.; Martin, H.; Guidoni, L. Effects of Static Correlation between Spin Centers in Multicenter Transition Metal Complexes. *J. Chem. Theory Comput.* **2017**, *13*, 4675–4683.
- [43] Montgomery, J. M.; Mazziotti, D. A. Strong Electron Correlation in Nitrogenase Cofactor, FeMoco. *J. Phys. Chem. A* **2018**, *122*, 4988–4996.
- [44] Barbatti, M.; Paier, J.; Lischka, H. Photochemistry of ethylene: A multireference configuration interaction investigation of the excited-state energy surfaces. *J. Chem. Phys.* **2004**, *121*, 11614–11624.
- [45] Yost, S. R.; Kowalczyk, T.; Van Voorhis, T. A multireference perturbation method using non-orthogonal Hartree-Fock determinants for ground and excited states. *J. Chem. Phys.* **2013**, *139*, 174104.
- [46] Sundstrom, E. J.; Head-Gordon, M. Non-orthogonal configuration interaction for the calculation of multielectron excited states. *J. Chem. Phys.* **2014**, *140*, 114103.
- [47] Loos, P.-F.; Scemama, A.; Blondel, A.; Garniron, Y.; Caffarel, M.; Jacquemin, D. A Mountaineering Strategy to Excited States: Highly Accurate Reference Energies and Benchmarks. *J. Chem. Theory Comput.* **2018**, *14*, 4360–4379.

- [48] Kato, T. On the eigenfunctions of many-particle systems in quantum Mechanics. *Comm. Pure Appl. Math.* **1957**, *10*, 151–177.
- [49] Borden, W.; Davidson, E. The Importance of Including Dynamic Electron Correlation in ab Initio Calculations. *Acc. Chem. Res.* **1996**, *29*, 67.
- [50] London, F. *Z. Physik. Chem. B* **1930**, *11*, 222–251.
- [51] Pople, J. A.; Nesbet, R. K. Self-consistent orbitals for radicals. *J. Chem. Phys.* **1954**, *22*, 571–572.
- [52] Awoonor-Williams, E.; Isley III, W. C.; Dale, S. G.; Johnson, E. R.; Yu, H.; Becke, A. D.; Roux, B.; Rowley, C. N. Quantum Chemical Methods for Modeling Covalent Modification of Biological Thiols. *J. Comput. Chem.* **2019**, *41*, 33–83.
- [53] Cohen, A. J.; Mori-Sánchez, P.; Yang, W. Insights into Current Limitations of Density functional Theory. *Science* **2008**, *321*, 792–793.
- [54] Foulkes, W. M. C.; Mitas, L.; Needs, R. J.; Rajagopal, G. Quantum Monte Carlo simulations of solids. *Rev. Mod. Phys.* **2001**, *73*, 33–83.
- [55] Szalay, P. G.; Müller, T.; Gidofalvi, G.; Lischka, H.; Shepard, R. Multiconfiguration Self-Consistent Field and Multireference Configuration Interaction Methods and Applications. *Chem. Rev.* **2012**, *112*, 108–181.
- [56] Dalgaard, E.; Jørgensen, P. Optimization of orbitals for multiconfigurational reference states. *J. Chem. Phys.* **1978**, *69*, 3833–3844.
- [57] Yeager, D. L.; Jørgensen, P. Convergency studies of second and approximate second order multiconfigurational Hartree–Fock procedures. *J. Chem. Phys.* **1979**, *71*, 755–760.
- [58] Werner, H.; Meyer, W. A quadratically convergent multiconfiguration–self-consistent field method with simultaneous optimization of orbitals and CI coefficients. *J. Chem. Phys.* **1980**, *73*, 2342–2356.

- [59] Lengsfeld, B. H. General second [U+2010] order MCSCF theory for large CI expansions. *J. Chem. Phys.* **1982**, *77*, 4073–4083.
- [60] Roos, B. O. A new method for large-scale CI calculations. *Chem. Phys. Lett.* **1972**, *15*, 153–159.
- [61] Roos, B. O. The complete active space SCF method in a fock-matrix-based super-CI formulation. *Int. J. Quantum Chem.* **1980**, *18*, 175–189.
- [62] Siegbahn, P. E. M.; Almlöf, J.; Heiberg, A.; Roos, B. O. The complete active space SCF (CASSCF) method in a Newton–Raphson formulation with application to the HNO molecule. *J. Chem. Phys.* **1981**, *74*, 2384–2396.
- [63] Hirao, K. Multireference Möller-Plesset Method. *Chem. Phys. Lett.* **1992**, *190*, 374–380.
- [64] Hirao, K. *Chem. Phys. Lett.* **1993**, *201*, 59–66.
- [65] Nakano, H.; Nakayama, K.; Hirao, K.; Dupuis, M. *J. Chem. Phys.* **1997**, *106*, 4912–4917.
- [66] Hashimoto, T.; Nakano, H.; Hirao, K. *J. Mol. Struct.* **1998**, *451*, 25–33.
- [67] Andersson, K.; Malmqvist, P.; Roos, B. O.; Sadlej, A. J.; Wolinski, K. Second-Order Perturbation Theory with a CASSCF Reference Function. *J. Phys. Chem.* **1990**, *94*, 5483–5488.
- [68] Andersson, K.; Malmqvist, P.; Roos, B. O. Second-Order Perturbation Theory with a Complete Active Space Self-Consistent Field Reference Function. *J. Chem. Phys.* **1992**, *96*, 1218.
- [69] Andersson, K. Different forms of the zeroth-order Hamiltonian in second-order perturbation theory with a complete active space self-consistent field reference function. *Theor. Chim. Acta* **1995**, *91*, 31–46.

- [70] Pulay, P. A Perspective on the CASPT2 Method. *Int. J. Quantum Chem.* **2011**, *111*, 3273–3279.
- [71] Voorhis, T. V.; Head-Gordon, M. Benchmark variational coupled cluster doubles results. *J. Chem. Phys.* **2000**, *113*, 8873–8879.
- [72] Robinson, J. B.; Knowles, P. J. Application of the quasi-variational coupled cluster method to the nonlinear optical properties of model hydrogen systems. *J. Chem. Phys.* **2012**, *137*, 054301–0543013.
- [73] Bulik, I. W.; Henderson, T. M.; Scuseria, G. E. Can Single-Reference Coupled Cluster Theory Describe Static Correlation? *J. Chem. Theory Comput.* **2015**, *11*, 3171–3179.
- [74] Ramos-Cordoba, E.; Lopez, X.; Piris, M.; Matito, E. H<sub>4</sub>: A challenging system for natural orbital functional approximations. *J. Chem. Phys.* **2015**, *143*, 164112–164119.
- [75] Ivanic, J.; Ruedenberg, K. *Theor. Chem. Acc.* **2001**, *106*, 339–351.
- [76] Helgaker, T.; Jorgensen, P.; Olsen, J. *Molecular Electronic-Structure Theory*; John Wiley & Sons Ltd: New York, 2013.
- [77] Stoyanova, A.; Teale, A. M.; Toulouse, J.; Helgaker, T.; Fromager, E. Alternative separation of exchange and correlation energies in multi-configuration range-separated density-functional theory. *J. Chem. Phys.* **2013**, *139*, 134113.
- [78] Manni, G. L.; Carlson, R. K.; Luo, S.; Ma, D.; Olsen, J.; Truhlar, D. G.; Gagliardi, L. Multiconfiguration Pair-Density Functional Theory. *J. Chem. Theory Comput.* **2014**, *10*, 3669–3680.
- [79] Hedegård, E. D.; Olsen, J. M. H.; Knecht, S.; Kongsted, J.; Jensen, H. J. A. Polarizable embedding with a multiconfiguration short-range density functional theory linear response method. *J. Chem. Phys.* **2015**,
- [80] Garza, A.; Bulik, I.; Henderson, T.; Scuseria, G. Synergy between pair coupled cluster doubles and pair density functional theory. *J. Chem. Phys.* **2015**, *142*, 044109.

- [81] Gagliardi, L.; Truhlar, D. G.; Manni, G. L.; Carlson, R. K.; Hoyer, C. E.; Bao, J. L. Multiconfiguration Pair-Density Functional Theory: A New Way To Treat Strongly Correlated Systems. *Acc. Chem. Res.* **2017**, *50*, 66–73.
- [82] Goedecker, S.; Umrigar, C. J. Natural Orbital Functional for the Many-Electron Problem. *Phys. Rev. Lett.* **1998**, *81*, 866–869.
- [83] Sokolov, A. Y.; Schaefer III, H. F. Orbital-optimized density cumulant functional theory. *J. Chem. Phys.* **2013**, *139*, 204110.
- [84] Piris, M. A natural orbital functional based on an explicit approach of the two-electron cumulant. *Int. J. Quantum Chem.* **2012**, *113*, 620.
- [85] Hollett, J. W.; Hosseini, H.; Menzies, C. A cumulant functional for static and dynamic correlation. *J. Chem. Phys.* **2016**, *145*, 084106.
- [86] Rohr, D. R.; Toulouse, J.; Pernal, K. Combining density-functional theory and density-matrix-functional theory. *Phys. Rev. A* **2010**, *82*, 052502.
- [87] Piris, M. Interacting pairs in natural orbital functional theory. *J. Chem. Phys.* **2014**, *141*, 044107.
- [88] Colle, R.; Salvetti, O. Approximate calculation of the correlation energy for closed shells. *Theor. Chim. Acta* **1975**, *37*, 329.
- [89] Hollett, J. W.; Pegoretti, N. On-top density functionals for the short-range dynamic correlation between electrons of opposite and parallel spin. *J. Chem. Phys.* **2018**, *148*, 164111–164119.
- [90] Hollett, J. W.; Loos, P.-F. Capturing static and dynamic correlation with  $\Delta$ NO-MP2 and  $\Delta$ NO-CCSD. *J. Chem. Phys.* **2020**, *152*, 014101.
- [91] Colle, R.; Salvetti, O. Approximate Calculation of the Correlation Energy for the Closed and Open Shells. *Theoret. Chim. Acta* **1979**, *53*, 55–63.

- [92] Kutzelnigg, W.; Mukherjee, D. Cumulant expansion of the reduced density matrices. *J. Chem. Phys.* **1999**, *110*, 2800.
- [93] Roach, P. J., A. C. Kuntz Unified large basis set diatomics-In-molecules models for ground and excited states of H<sub>3</sub>. *J. Chem. Phys.* **1985**, *84*, 822.
- [94] Burton, H. G. A.; Thom, A. J. W. Holomorphic Hartree–Fock Theory: An Inherently Multireference Approach. *J. Chem. Theory Comput.* **2016**, *12*, 167–173.
- [95] Mori-Sánchez, J. A., Paula Cohen Qualitative breakdown of the unrestricted Hartree-Fock energy. *J. Chem. Phys.* **2014**, *141*, 164124.
- [96] Bokes, P.; Štich, I.; Mitas, L. Electron correlation effects in ionic hydrogen clusters. *Int. J. Quantum Chem.* **2001**, *83*, 86–95.
- [97] Schmidt, M. W.; Baldridge, K. K.; Boatz, J. A.; Elbert, S. T.; Gordon, M. S.; Jensen, J. H.; Koseki, S.; Matsunaga, N.; Nguyen, K. A.; Su, S.; et al., *J. Comput. Chem.* **1993**, *14*, 1347–1363.
- [98] Poirier, R. A.; Hollett, J. W.; Warburton, P. L. MUNgauss. Memorial University, Chemistry Department, St. John’s, NL A1B 3X7, 2015; With contributions from A. Alrawashdeh, J.-P. Becker, J. Besaw, S.D. Bungay, F. Colonna, A. El-Sherbiny, T. Gosse, D. Keefe, A. Kelly, D. Nippard, C.C. Pye, D. Reid, K. Saputantri, M. Shaw, M. Staveley, O. Stueker, Y. Wang, and J. Xidos.
- [99] Dunning Jr., T. H. Gaussian Basis Sets for Use in Correlated Molecular Calculations. I. The Atoms Boron Through Neon and Hydrogen. *J. Chem. Phys.* **1989**, *90*, 1007.
- [100] Kendall, R. A.; Dunning Jr., T. H. Electron Affinities of the First-Row Atoms Revisited. Systematic Basis Sets and Wave Functions. *J. Chem. Phys.* **1992**, *96*, 6796–6806.
- [101] Woon, D. E.; Dunning Jr., T. H. Gaussian basis sets for use in correlated molecular calculations. IV. Calculation of static electrical response properties. *J. Chem. Phys.* **1994**, *100*, 2975–2988.

# Chapter 3

## Summary and Future work

A major aspect of theoretical chemistry is making computational chemistry, *i.e.*, the algorithms behind the models, faster and more accurate. The number of developed computational methods extends through the years to solve the problems that were or still are present. Although to some scientists some issues were alleviated, like dispersion interactions, to others it is still present; however, partial solutions were provided. Different electronic structure methods deal well with finding the ground state energy and studying specific properties of bond lengths, band gaps, charge transfer, to name a few. Excited states, however, remain challenging, but insights in some systems were provided using time-dependent density-functional theory (TDDFT). Other challenges include static correlation, which is still a significant one.

Various methods were dedicated to solving the issue of static correlation while accounting for dynamic correlation as well; however, it seems that whether it is accuracy that fails to a specific point, the computational cost that tends to be expensive, or the difficulty of the code to implement and test that makes some methods excruciating if not impossible to use. For example, Becke 13 (B13) functional provided a solution to static correlation; however, the functional is complicated and has not been coded for self-consistent optimization, *i.e.*, Kohn–Sham equations. Some implementations, such as multiconfiguration pair-density functional theory (MC-PDFT) and pair coupled cluster doubles (pCCD), seem successful; however, testing remains the final outcome that shows whether a method is tackling the

static correlation challenge or not. Among these successful methods and theories,  $\Delta$ NO saw light and is going through the testing section. It is a fact that has been presented in this work that the performance of the functional is robust when it comes to systems that are statically correlated.  $\Delta$ NO accounts for dynamic correlation energies through dynamic correlation functionals. The pairing used in  $\Delta$ NO is sufficient to account for the needed qualitative description of the investigated hydrogen clusters.

The analysis of the PES of hydrogen clusters studied led to a novel derivation of an efficient  $\Delta$ NO theory. In fact, investigating these hydrogen clusters aided in understanding the pairing of the orbitals needed not only for the studied clusters, but also the future works of some systems like twisted ethylene that can be modelled much easier than, for example, square to rectangle  $H_4$ . However, the selection of the NOs that needs to be paired in order to describe a system properly remains a crucial part that needs improvement in the method. This idea itself may have been developed or undergoing development through machine learning, however, doing that requires a numerous amount of work, training, and collecting data for the code. An idea originated in the Hollett group that will be developed in the upcoming future that pairs the NOs based on momentum-balanced density. As a matter of fact, achieving this idea and making it a reality and implementing into other codes like GAMESS is by itself a milestone to electronic structure theory.  $\Delta$ NO is attractive to use not only due to its superb performance but also its cheap computational cost that scales to  $N_{act}K^4$ , where  $N_{act}$  is the active space or pairing of NOs and  $K^4$  is the basis functions.

The systems investigated herein seem simple in structure to chemists, however, it has proven that it is more than that. The simple number of orbitals and their pairing provide an idea how a larger molecule can actually be easier to model, for example, working on stretching the square  $H_4$  with the premium performance of  $\Delta$ NO shows how systems of a similar geometry but larger number of electrons and nuclei, like cyclobutadiene, can be studied somewhat easier.

To conclude, this work has presented significantly challenging systems to electronic structure methods of one- and two-dimensional hydrogen clusters. In general, the predicted ener-

gies of linear hydrogen cluster over their studied PESs mimic the ones computed at full CI, unlike conventional electronic structure methods, where it fails in dealing with them, particularly, the  $H_4$  ( $D_{4h}$ ) cluster. The  $\Delta$ NO predicted potential energies of  $H_4$   $D_{2h} \rightarrow D_{4h} \rightarrow D_{2h}$  are qualitatively smooth, which means that  $\Delta$ NO captures static correlation properly. Furthermore, the energies are comparable to full CI at certain bond lengths. There is still further work required to test the method and provide insights into different challenges, ground state systems for now, and excited states in the future.

# Appendix A

## Appendix

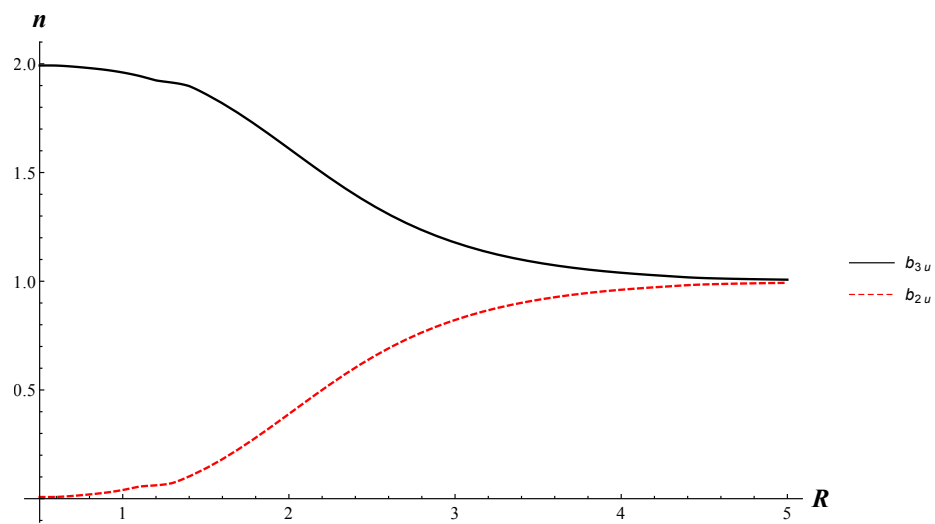


Figure A.1: Change of occupation numbers of statically correlated NOs of  $H_4$  as a function of  $R$ .

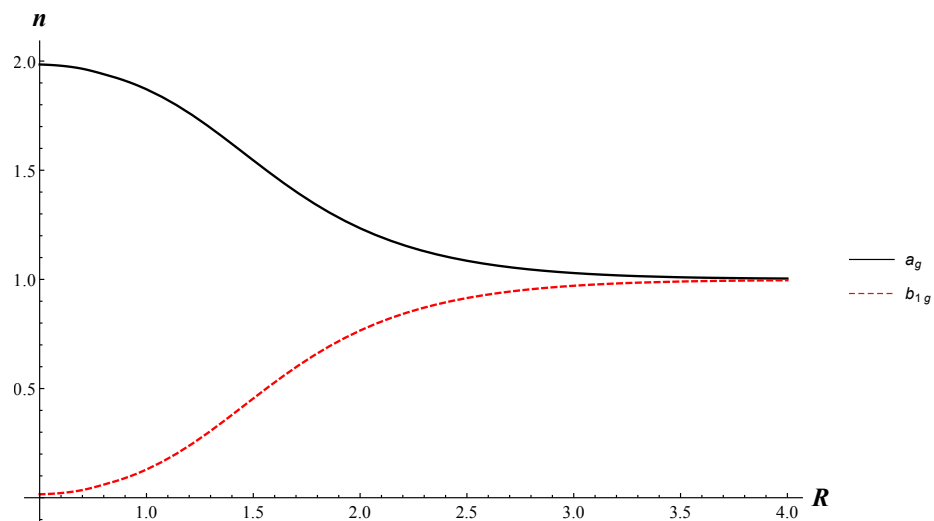


Figure A.2: Change of occupation numbers of statically correlated NOs of square  $H_4$  ( $D_{4h}$ ) as a function of  $R$ .

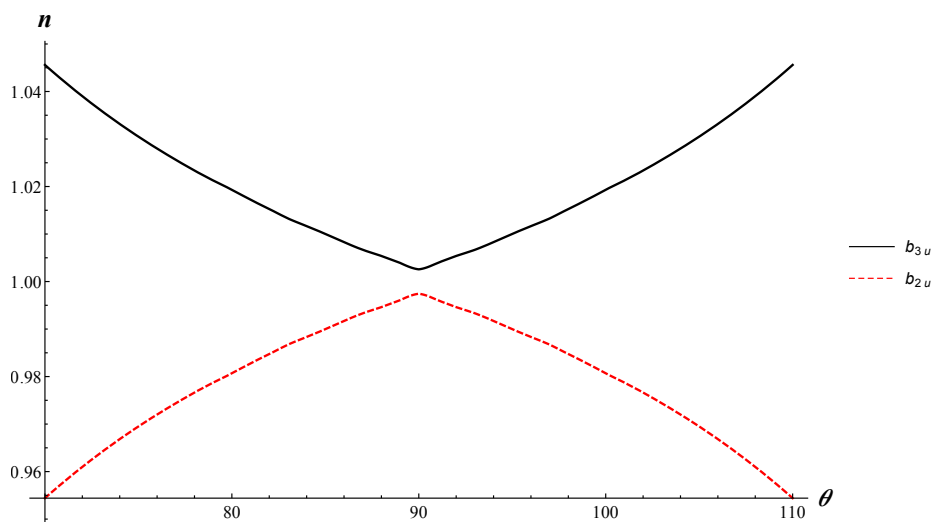


Figure A.3: Change in occupation numbers of statically correlated NOs of  $H_4$  ( $D_{2h}/D_{4h}$ ) as a function of  $\theta$ ,  $R = 3.0 \text{ \AA}$ .

Table A.1: Absolute energy values (hartree) for  $H_4$  ( $D_{2h}/D_{4h}$ ) at different  $\theta$  and  $R$  values.

$\theta^\circ$	$R = 0.8 \text{ \AA}$			$R = 1.0 \text{ \AA}$			$R = 1.2 \text{ \AA}$		
	Full CI	$\Delta\text{NO-CS}$	$\Delta\text{NO-OF}$	Full CI	$\Delta\text{NO-CS}$	$\Delta\text{NO-OF}$	Full CI	$\Delta\text{NO-CS}$	$\Delta\text{NO-OF}$
70	-2.216905602	-2.2026557874	-2.2150079363	-2.1984305684	-2.202656331	-2.1968989698	-2.1484699306	-2.1520092598	-2.1480953094
72	-2.2050940721	-2.1893289446	-2.2025256956	-2.1858734613	-2.189330732	-2.1837663206	-2.1370707346	-2.1399553054	-2.1363685642
74	-2.1928193673	-2.1759771286	-2.1894886101	-2.173412357	-2.1759786356	-2.1706246543	-2.1261357759	-2.128241501	-2.1250009607
76	-2.1801727759	-2.162628619	-2.1759497669	-2.1611142775	-2.1626170074	-2.1574907954	-2.1157049075	-2.1168662538	-2.1139843947
78	-2.1672568412	-2.1492687909	-2.1619550837	-2.1490646143	-2.1492587651	-2.1443771187	-2.1058344673	-2.1058115573	-2.1032968942
80	-2.1542058783	-2.1359137718	-2.1475163896	-2.1373872991	-2.1359056508	-2.1312848952	-2.0966121356	-2.0950661693	-2.0929298892
82	-2.1412273116	-2.1225666468	-2.1326776607	-2.126282101	-2.1225539006	-2.1182098398	-2.0881817344	-2.0845896415	-2.0828455492
84	-2.1286926985	-2.1092174875	-2.1184742733	-2.1160949833	-2.1092174881	-2.1074138281	-2.0807829796	-2.0753740245	-2.0757568105
86	-2.1173460242	-2.1046350641	-2.1114996344	-2.1074409555	-2.1046350644	-2.1029279706	-2.0748036862	-2.0725703913	-2.0730379871
88	-2.1087163695	-2.1018558218	-2.1071606756	-2.1013433808	-2.101855822	-2.1002129173	-2.0708024056	-2.0708918478	-2.0714118294
90	-2.1053124985	-2.1009216109	-2.1056870945	-2.0990881493	-2.100924217	-2.099300704	-2.0693760973	-2.0703287874	-2.0708692365
	$R = 1.5 \text{ \AA}$			$R = 1.7 \text{ \AA}$			$R = 2.2 \text{ \AA}$		
70	-2.0777097905	-2.0814418667	-2.0800511417	-2.0452012814	-2.0491390123	-2.0489035411	-2.0086505483	-2.007178862	-2.0095182926
72	-2.0696381115	-2.0729645734	-2.0719967654	-2.0395376039	-2.0431749111	-2.0433074304	-2.007035659	-2.0060714723	-2.0084024078
74	-2.062256075	-2.0650920054	-2.0645388445	-2.0345179018	-2.0378001383	-2.0382834992	-2.0057038866	-2.005163869	-2.0074829379
76	-2.0555440025	-2.0577778933	-2.057630882	-2.0300907386	-2.0329516574	-2.0337667544	-2.004606425	-2.0044244194	-2.0067300315
78	-2.0494903049	-2.0509791782	-2.0512223407	-2.026212074	-2.0285405486	-2.0296905476	-2.0037032093	-2.0038273884	-2.0061190734
80	-2.0440986142	-2.0446305874	-2.045264433	-2.0228493049	-2.0245051971	-2.0259940209	-2.0029622859	-2.0033521947	-2.0056308508
82	-2.0393986582	-2.0386906903	-2.039704665	-2.0199872995	-2.0208689437	-2.0226629061	-2.0023597291	-2.0029826452	-2.0052499418
84	-2.0354618208	-2.0339651431	-2.0363868547	-2.0176372346	-2.0179890371	-2.0208333982	-2.0018805269	-2.002706684	-2.0049648163
86	-2.0324181004	-2.032666366	-2.0351328336	-2.0158470054	-2.0172243978	-2.0200898661	-2.0015208592	-2.0025154913	-2.0047670138
88	-2.0304568558	-2.0318954209	-2.034387026	-2.0147039342	-2.0167734105	-2.0196504464	-2.001290726	-2.002402841	-2.0046503591
90	-2.0297737326	-2.0316355652	-2.0341372268	-2.0143073745	-2.0166238149	-2.0195044211	-2.0012101794	-2.0023625062	-2.0046086622
	$R = 3.0 \text{ \AA}$								
70	-1.9998190925	-1.9999549111	-2.0010232552						
72	-1.9996896119	-1.9998172615	-2.0008252622						
74	-1.999591737	-1.9997094544	-2.0006629828						
76	-1.9995176063	-1.9996254222	-2.0005304294						
78	-1.9994613423	-1.9995603232	-2.0004228246						
80	-1.9994185683	-1.9995105053	-2.0003369961						
82	-1.9993860663	-1.9994725809	-2.0002689205						
84	-1.9993615683	-1.9994450287	-2.000218013						
86	-1.9993437155	-1.9994261777	-2.0001823507						
88	-1.9993322506	-1.9994149644	-2.0001611466						
90	-1.9993281434	-1.9994106978	-2.0001534526						

Table A.2: The difference in absolute energies at  $\theta = 90^\circ$  and  $70^\circ$  ( $\text{kJ mol}^{-1}$ ) for  $\text{H}_4$  ( $D_{2h}/D_{4h}$ ).

$R$ ( $\text{\AA}$ )	Full CI	B3LYP*	CCSD(T)*	$\Delta\text{NO-CS}$	$\Delta\text{NO-OF}$
0.8	293	381	287	267	287
1.0	261	369	244	267	256
1.2	208	333	180	214	203
1.5	126	268	88	131	121
1.7	81	227	45	85	77
2.2	20	142	3	13	13
3.0	1	63	—	1	2

\* Incorrect description of the PES. — Does not converge.